AD_____

Award Number: DAMD17-03-1-0349

TITLE: Tissue Microarray Based Investigation of Stat3 Signaling Pathway in Breast Cancer

PRINCIPAL INVESTIGATOR: Marisa Dolled-Filhart

CONTRACTING ORGANIZATION: Yale University
New Haven, CT 06520-8047

REPORT DATE: May 2004

TYPE OF REPORT: Annual

PREPARED FOR: U.S. Army Medical Research and Materiel Command
Fort Detrick, Maryland 21702-5012

DISTRIBUTION STATEMENT: Approved for Public Release;
Distribution Unlimited

REPORT DOCUMENTATION PAGE

Form Approved
OMB No. 074-0188

1. AGENCY USE ONLY (Leave blank)	2. REPORT DATE	3. REPORT TYPE AND DATES COVERED
	May 2004	Annual (1 May 2003 - 30 Apr 2004)

4. TITLE AND SUBTITLE

Tissue Microarray Based Investigation of Stat3 Signaling Pathway in Breast Cancer

5. FUNDING NUMBERS

DAMD17-03-1-0349

6. AUTHOR(S)

Marisa Dolled-Filhart

7. PERFORMING ORGANIZATION NAME(S) AND ADDRESS(ES)

Yale University
New Haven, CT 06520-8047

E-Mail: marisa.dolled@yale.edu

8. PERFORMING ORGANIZATION REPORT NUMBER

9. SPONSORING / MONITORING AGENCY NAME(S) AND ADDRESS(ES)

U.S. Army Medical Research and Materiel Command
Fort Detrick, Maryland 21702-5012

10. SPONSORING / MONITORING AGENCY REPORT NUMBER

11. SUPPLEMENTARY NOTES

12a. DISTRIBUTION / AVAILABILITY STATEMENT

Approved for Public Release; Distribution Unlimited

12b. DISTRIBUTION CODE

13. ABSTRACT (Maximum 200 Words)

The objective of this proposal is to identify fingerprints or "keystone" markers based on clinical outcome using tissue microarrays (TMAs) and automated analysis (AQUA). This is a novel method that will allow the identification of "prognosis fingerprints" important in disease-specific breast cancer survival. While the original proposal focused on construction of only lymph node-negative tissue microarrays, node-positive specimens have been included to help find markers that can separate patients based on their nodal status and to assist in the discovery of biomarkers important in a "prognosis" signature for breast cancer regardless of nodal status. As of this progress report, we have completed the construction of the tissue microarrays, the collection of the clinical data for the cohort, and the assessment of the tissue microarrays with standard clinical biomarker antibodies (ER, PR, Her2 and Ki-67). We are currently in the process of analyzing over 40 biomarkers on the tissue microarrays by AQUA for their prognostic value individually, and multiplexed with other biomarkers and clinicopathological data, in order to determine which biomarkers are key in subclassifying the breast cancer tumor cohort.

14. SUBJECT TERMS

Breast cancer

15. NUMBER OF PAGES

47

16. PRICE CODE

17. SECURITY CLASSIFICATION OF REPORT	18. SECURITY CLASSIFICATION OF THIS PAGE	19. SECURITY CLASSIFICATION OF ABSTRACT	20. LIMITATION OF ABSTRACT
Unclassified	Unclassified	Unclassified	Unlimited

Table of Contents

Introduction:

In this study we proposed a potential method for rapid evaluation of biomarkers and their relationship to breast cancer survival in node-negative breast cancer cases by evaluation of breast cancer cohort tissue microarrays. Tissue microarrays consist of 0.6 mm diameter samples of breast cancers from hundreds of patients on a single slide in a grid format that allows each tumor to be linked to its clinical information. Using this method, we proposed high throughput screening for potential biomarkers of the Stat3 signaling pathway in order to identify fingerprints or "keystone" markers based on clinical outcome and automated analysis (AQUA). AQUA is a set of algorithms developed in our laboratory that allows for rapid quantitative analysis of immunofluorescence on tissue microarrays. The results of the quantitative analysis by AQUA would allow for clustering analyses in order to molecular classify tumors based on their protein expression of the large number of biomarkers assessed in this study.

Body:

The proposed goal of this study was to identify node-negative tumors with a poor outcome based on the expression of new potiential biomarkers by looking at markers up and down the Stat3 signaling pathway. While we had some interesting results in node-negative tumors looking at Stat3 and Phospho-Stat3 (Dolled-Filhart, et al 2003), we realized early on that this approach with single biomarkers in one signaling pathway was too limited. As the global goal is to classify tumors, we felt we needed to look beyond Stat3 signaling and to take advantage of new data of potential biomarkers emerging from cDNA microarrays in order to better separate out patients with a poor prognosis. cDNA microarrays of breast cancer are a rich and so far, relatively untapped, resource for exploring the relationship of new biomarkers, either singly or multiplexed, with patient outcome. Additionally, we thought more about our use of only node-negative specimens, as it is not actually a disease classification. Historically, about 30% of node-negative patients to further disease, suggesting that nodal status is a good surrogate of patient survival but not the ultimate discriminator of patient outcome. Therefore, we felt that we had the opportunity to stratify patients of both node-negative and node-positive status using multiple new biomarkers and our tissue microarray and AQUA technologies. This study has been extended to include a cohort of both node-negative and node-positive patients in a high-throughput manner, utilizing a tissue microarray of 250 breast cancer cases (125 node-negative and 125 node-positive). This will allow us the most power in molecularly classifying those patients with poor prognosis from the rest of the patients for a wide range of proteins in a wide range of functions, as well as to assess differences in expression between tumors of different nodal status.

We originally proposed the following specific aims:

(1) Creation of lymph node negative primary breast cancer tumor TMAs and validation with standard clinical biomarkers

(2) Selection of Stat3 signaling components and protein expression analysis on TMAs by AQUA. (3) Clustering analysis of the Stat3 signaling components to define "keystone" markers and validate their classifying strength on the basis of prognostic value.

The original Statement of Work was as follows:

Task 1: Creation of lymph node negative primary breast cancer tumor tissue microarrays (Months 1-3)

a. Select 350 lymph node-negative invasive primary breast carcinoma tumors from the Yale Pathology archives that were resected between 1960 and 1980.
b. Review with a pathologist the sections of invasive breast carcinoma and mark the regions of the tumor that will be used for the tissue microarray.
c. Create the tissue microarray with two replicate tissue microarrays.

Task 2: Evaluation of the tissue microarrays with standard clinical biomarkers and creation of a database of clinical information. (Months 3-6)

a. Use standard clinical biomarker antibodies for immunofluorescence to stain the tissue microarray with ER, PR, Her2 and Ki-67
b. Determine the protein expression levels of the above markers in each tumor using AQUA software
c. Set up and populate a database of the associated clinical information using the precise grid format of the tissue microarray construction to link each tumor to its clinical parameters.

Task 3: Evaluation of Stat3 and its signaling pathway components' protein expression on the cohort and determination of prognostic value. (Months 6-30)

a. Use commercially available antibodies for Stat3 and its signaling components for immunofluorescence on the tissue microarrays
b. Determine the protein expression levels of the different components for each tumor using AQUA
c. Determine the prognostic value of the different components utilizing Kaplan-Meier survival curves, univariate and multivariate analysis in conjunction with the clinical information in the database.

Task 4: Determination of subclassifications ("fingerprints") and critical targets "keystones" of Stat3 signaling components in breast cancer (Months 12-36)

a. Clustering analysis based on expression levels but inclusive of patient outcome data.
b. Determination of which components are key in subclassifying the tumors.

This progress report describes work completed in the first year.

Task 1 was successfully completed during the first year. Tissue microarrays consisting of lymph node-negative invasive primary breast carcinoma tumors from the Yale Pathology archives that were resected between 1960 and 1980 were constructed after sections of invasive carcinoma were marked by a pathology. Replicate tissue microarrays were constructed. In addition, the tissue microarrays also include lymph node-positive invasive primary breast carcinoma tumors from the Yale Pathology archives that were resected between 1960 and 1980, also with invasive sections chosen by a pathologist. Furthermore, a tissue microarray consisting of half node-

positive tumor and half node-negative tumors (250 cases total) was constructed with replicates so that there would be tissues microarray slides available for high throughput analysis of many biomarkers.

Task 2 was successfully completed during the first year. The breast cancer cohort was assess with standard clinical biomarkers with antibodies to estrogen receptor, progesterone receptor, Her-2-neu and Ki-67 by immunofluorescence and quantitated by AQUA. Additionally, there is a database that has been created that houses the associated clinical information for each specimen in the tissue microarrays that was also constructed to house the data from the AQUA analyses. A paper describing the results of the Her-2-neu analysis on the node-positive samples by automated analysis is included in the appendix (Camp et al, 2003).

Task 3 was begun with an assessment of Stat3 and Phospho-Stat3 on the lymph-node negative breast cancer specimens using manual scoring as we were still finalizing the AQUA methods for tissue microarrays. The paper describing the AQUA method that was finalized in our lab is included in the appendix (Camp et al, 2002). The resulting published paper is included in the appendix (Dolled-Filhart, et al 2003). Additionally, a significant amount of time was spent writing a book chapter on the levels of Stats in tumors for *Signal Transducers and Activators of Transcription* which is included in the appendix (Dolled-Filhart and Rimm, 2003). As mentioned above, the selection of biomarkers has been changed from the Stat3 signaling pathway to allow for leverage of new data on biomarkers resulting from many large scale cDNA microarray analyses of breast cancer cases. We are currently in the process of assessing upwards of 40 different biomarkers by AQUA in order to quantitate the protein expression levels of these markers in the breast cancer tissue microarrays. The biomarkers will be done in the same manner as originally proposed, and analyzed for prognostic value as originally proposed in Task 3. However, the actual biomarkers used will be different from those originally described to take into account recent advances in breast cancer profiling studies. Each biomarker will be assessed individually for prognostic value in univariate analysis, as well as in multivariate analysis.

Task 4, which is the determination of outcome-based subclassifications "fingerprints" in breast cancer, has been expanded from the original statement of work. We plan to cluster and multiplex the large number of markers mentioned in the Task 3 progress in order to meet the proposed goal of quantitative molecular subclassification of breast cancer tumors by patient outcome by using a large number of potential biomarkers. The methods for this type of analysis are currently being explored and once determined, will be applied to the data collected from Task 3.

Key Research Accomplishments:

- Completion tissue microarray construction
- Completion of a database with patient cohort information
- Completion of assessment of the tissue microarray with standard clinical biomarkers

Reportable Outcomes:
Analysis of Stat3 and PhosphoSTat3 shows that they are predictive of outcome in node-negative breast cancer tumors as a potential marker of improved survival independent of other prognostic markers.

Conclusions:
Tissue microarrays are a valuable tool for analysis of new potential biomarkers in breat cancer when coupled with automated quantitative analysis. Completion of quantitative analysis of upwards of 40 biomarkers on a large cohort of breast cancer specimens will allow for new and interesting outcome-based molecular subclassification of breast cancer samples. The use of the 40 biomarkers derived from current cDNA microarray profiling studies of breast cancer, rather than solely the Stat3 signaling pathway components, will allow for a broad assessment of novel potential biomarkers that can better help us reach the goal of outcome-based classification of breast cancer specimens. We anticipate evaluation of all of the biomarkers within the next year, which would be well within the expected time-line for completion of Task 3, and for analysis of the biomarkers as per Task 4 in the following year.

References:
See original proposal.

Appendices:

1. Dolled-Filhart M, Camp RL, Kowalski DP, Smith BL, Rimm DL. *Tissue Microarray Analysis of Signal Transducers and Activators of Transcription 3 (Stat3) and Phospho-Stat3 (Tyr705) in Node-negative Breast Cancer Shows Nuclear Localization Is Associated with a Better Prognosis.* Clinical Cancer Research. 2003 Feb;9(2):594-600.

2. Dolled-Filhart, M. and Rimm, D.L. *JAKs/STATs as Biomarkers of Disease*, in "Signal Transducers and Activators of Transcription (STATs): Activation and Biology. Volume editors PB Sehgal, DE Levy and T Hirano. (2003) p.697-720

3. Camp, R.L. Chung, G.G., and Rimm, D.L. (2002) *Algorithms for Automated Tissue Microarray Analysis Reveal Novel Disease Sub-classifications.* Nature Medicine 8(11):1323-8

4. Camp, R.L., Dolled-Filhart, M., King, B and Rimm, D.L. (2003) *Quantitative Analysis of Breast Cancer Tissue Microarrays Shows That Both High and Normal Levels of HER2 Expression Are Associated with Poor Outcome.* Cancer Research 63:1445-1448.

594 Vol. 9, 594–600, February 2003 Clinical Cancer Research

Advances in Brief

Tissue Microarray Analysis of Signal Transducers and Activators of Transcription 3 (Stat3) and Phospho-Stat3 (Tyr705) in Node-negative Breast Cancer Shows Nuclear Localization Is Associated with a Better Prognosis[1]

Marisa Dolled-Filhart, Robert L. Camp, Diane P. Kowalski, Bradley L. Smith, and David L. Rimm[2]

Department of Pathology, Yale University School of Medicine, New Haven, Connecticut 06510 [M. D-F., R. L. C., D. P. K., D. L. R.], and Cell Signaling Technology, Beverly, Massachusetts [B. L. S.]

Abstract

Purpose: **Although a high frequency of tumors contain constitutively activated signal transducers and activators of transcription 3 (Stat3), its relationship to breast cancer and patient survival has not been determined in a large retrospective study of node-negative tumors. To further elucidate the role of Stat3 in breast cancers, the expression patterns of Stat3 and Phospho-tyrosine residue 705 (Tyr705) Stat3 were correlated with survival outcome and clinicopathological parameters in a large cohort of node-negative breast cancer tumors.**

Experimental Design: **Immunohistochemical analysis of Stat3 and Phospho-Stat3 was performed on a breast cancer tissue microarray of 346 node-negative breast cancer specimens. These results were correlated with overall survival and other clinicopathological data.**

***Results*: Positive Stat3 cytoplasmic expression was seen in 69.2% of tumors, and positive Phospho-Stat3 (Tyr705) cytoplasmic expression was seen in 19.6% of tumors. Neither cytoplasmic expression showed significant association with survival or other clinical parameters. However, 23.1% of tumors had positive Stat3 nuclear expression, and those patients had a significantly improved short-term survival ($P = 0.0332$) at 5 years of follow-up. Upon analysis of positive Phospho-Stat3 (Tyr705) nuclear expression, seen in 43.5% of tumors, positive tumors had a significantly improved survival at both short-term 5-year survival ($P = 0.0054$) and long-term 20-year ($P = 0.0376$) survival analysis. Additionally, positive Phospho-Stat3 (Tyr705) nuclear expression is an independent prognostic marker of better overall survival node-negative breast cancer by multivariate analyses that included the variables of nuclear grade, Ki-67, estrogen receptor staining, progesterone receptor staining, Her2 staining, age, and tumor size.**

Conclusions: **These findings support a role for Stat3 and Phospho-Stat3 (Tyr705) overexpression in node-negative breast cancer and provide initial evidence that Phospho-Stat3 (Tyr705) may be a marker for improved overall survival independent of other prognostic markers.**

Introduction

Stat[3] proteins are transcription factors that are activated by a wide range of cytokine receptor-associated kinases, growth factor receptor tyrosine kinases, and nonreceptor tyrosine kinases originally defined as the signaling mechanism for IFN receptors (1). Stat3 has posed a special challenge because, unlike other Stat proteins, it shows an embryonic lethal phenotype (2). This has complicated characterization of its function and, in part, led to some controversy regarding the role of Stat3 in tumors. Although there is some evidence that it is an oncogene, there is also evidence that it behaves as a tumor suppressor (3).

Stat3, like other Stat proteins, contains an SH2 domain, which is a common motif found in signaling molecules that mediate protein-protein interactions by binding directly to specific phosphotyrosines. Stat3 is activated by phosphorylation of Tyr705 by c-Jun NH_2-terminal kinases, growth factor tyrosine kinases, or other mechanisms (4). Phosphorylation precipitates dimerization, which is stabilized by reciprocal phospho-tyrosine SH2 interactions. Stat3 dimers then move to the nucleus, where they bind to specific DNA response elements in target gene promoters and enable gene transcription. Some target genes of Stat3 include those involved in apoptosis, cell cycle regulation, and induction of growth arrest such as Bcl-xL, cyclin D1, p21, WAF1/CIP1, and c-myc (5).

Because Stat3 plays such a pleomorphic role in signal transduction, its role as an oncogene or a tumor suppressor may be a function of the setting. In the context of the mouse mammary gland, Stat3 is activated both during apoptotic involution and during the highly proliferative phase of early pregnancy (6). Subsequent conditional knockout studies in mice have shown that Stat3 is essential in mammary gland epithelial cell apoptosis

Received 5/13/02; revised 9/19/02; accepted 9/30/02.
The costs of publication of this article were defrayed in part by the payment of page charges. This article must therefore be hereby marked *advertisement* in accordance with 18 U.S.C. Section 1734 solely to indicate this fact.
[1] Supported by grants from the Patrick and Catherine Weldon Donaghue Foundation for Medical Research, the United States Army (DAMD17-01-1-0463), and grants from the NIH, including RO-1 GM57604.
[2] To whom requests for reprints should be addressed, at Department of Pathology, Yale University School of Medicine, 310 Cedar Street, New Haven, CT 06510. Phone: (203) 737-4204; Fax: (203) 737-5089; E-mail: david.rimm@yale.edu.

[3] The abbreviations used are: Stat, signal transducers and activators of transcription; Tyr705, tyrosine residue 705; ER, estrogen receptor; PR, progesterone receptor; TBS, Tris-buffered saline.

and involution (7, 8). In humans, Stat3 is activated in several mammary epithelial cells and breast carcinoma cell lines (9–13). There is evidence of increased Stat binding in the nuclei of breast cancer tumors compared with normal breast tissue or benign lesions (14, 15). An immunohistochemical study of 62 cases of invasive malignant breast cancer tumors by Berclaz *et al.* (16) found that Stat3 was expressed only in the cytoplasm of nontumor regions of breast cancer specimens but was expressed in both the cytoplasm and nuclei of malignant regions of the specimens. However, they found no correlation between Stat3 subcellular localization expression and survival. Recently, an antibody specific for the activated (phospho-Tyr705) form of Stat3 has become available (17). In prostate tissue, the activated form of Stat3 localized predominantly to the nuclei of malignant glands (18). This activated form may be a better probe for function than total Stat3, but it has not yet been evaluated in breast cancer tissues.

Tissue microarray technology (19, 20) is a highly efficient and economical way to evaluate hundreds of tumors (21). Breast cancer is a common application of this technology. Breast cancer tissue microarray cores have been demonstrated to be representative of the conventional tumor specimens because as they have very high concordance for common biomarkers as well as reproducible prognostic associations (22–24) and recently reviewed (29). Results from validation studies have shown that in the majority of the cases, one tissue microarray core alone could adequately represent the antigen expression of the corresponding whole section and be representative of the association between the staining level and clinical end point (24). The use of archival tissue for a retrospective study allows for protein expression to be analyzed with the benefit of long-term followup (survival) information. Here, we evaluate the expression and subcellular localization of both Stat3 and Phospho-Stat3 (Tyr705) by immunohistochemistry in a tissue microarray containing a cohort of 346 node-negative archival-infiltrating breast cancer tumors. The expression and localization information were correlated with standard clinicopathological factors and with overall patient survival.

Materials and Methods

Tissue Microarray Construction. The tissue microarrays were constructed as previously described (20), with 0.6-mm diameter cores spaced 0.8 mm apart. Expression was evaluated on two arrays, including a validation array and a cohort array. The validation array, as previously described (22), was constructed with three replicate cores for each of the breast cancer cases. The validation array consisted of the following number of cases from each decade: 1930s (14 cases), 1940s (8 cases), 1950s (12 cases), 1960s (13 cases), 1970s (11 cases), 1980s (9 cases), and 1990s (15 cases). The cohort node-negative breast cancer array was constructed from paraffin-embedded formalin-fixed tissue blocks from the Yale University Department of Pathology archives. The specimens were resected between 1962 and 1980, with a follow-up range of patient breast cancer history between 4 months and 53.8 years, with a mean follow-up time of 15.6 years. Time between tumor resection and fixation was not available for the tumors in this cohort. Representative tumor regions were selected for coring and placement in the tissue microarray using a Tissue Microarrayer (Beecher Instruments, Silver Spring, MD). The tissue microarrays were then cut to 5-μm sections and placed onto slides by use of an adhesive tape-transfer system (Instrumedics, Inc., Hackensack, NJ) and UV cross-linking.

Immunohistochemistry. The tissue microarray slides were deparaffinized with xylene rinses and then transferred through two changes of 100% ethanol. Endogenous peroxidase activity was blocked by a 30-min incubation in a 2.5% hydrogen peroxide/methanol buffer. Antigen retrieval was performed by boiling the slides in a pressure cooker filled with a sodium citrate buffer (pH 6.0). After antigen retrieval, the slides were incubated with 0.3%BSA/1× TBS for 1 h at room temperature to reduce nonspecific background staining, followed by a series of 2-min rinses in 1× TBS, 1× TBS/0.01% Triton, and 1× TBS. Primary antibody was applied for 1 h at room temperature (1:100 dilution of Phospho-Stat (Tyr705) antibody (Cell Signaling Technology, Beverly, MA) in 0.3%BSA/1× TBS or 1:150 dilution of Stat3 antibody (Cell Signaling Technology) in 0.3%BSA/1× TBS). After a series of TBS rinses as described above, bound antibody was detected by using an antirabbit horseradish peroxidase-labeled polymer secondary antibody from the Dako Envision TM + System (Dako, Carpinteria, CA). The slides were rinsed in the TBS series, visualized with a 10-min incubation of liquid 3,3′-diaminobenzidine in buffered substrate (Dako) for 10 min. Finally, the slides were counterstained with hematoxylin and mounted with Immunomount (Shandon, Pittsburgh, PA). Immunohistochemical staining was also done for ER, PR, and Her2 as described previously (22). Ki-67 expression was assessed using purified antihuman monoclonal antibody (1:200, overnight incubation; PharMingen, San Diego, CA).

Evaluation of Immunohistochemical Staining. For each spot, the regions of most intense and/or predominant staining pattern were scored by eye. Traditionally, immunohistochemistry scoring of stain intensity includes a variable for the area percentage stained with the specimen, but because of the small size of the spot (0.6 mm in diameter), no area variable is included. The nuclear and cytoplasmic staining was determined separately for each specimen. The staining intensity was graded on the following scale: 0, no staining; 1, weak staining; 2, moderate staining; and 3, intense staining. For specimens that were uninterpretable or were not infiltrating carcinoma, a score of not applicable (N/A) was given. Scoring of the tissue microarray was completed by two independent observers (M. D. F. and D. K.), with very high correlation between scorers ($P < 0.0001$) for both of the Stat3 cytoplasmic and nuclear localization scores and for both of the Phospho-Stat3 (Tyr705) cytoplasmic and nuclear localization scores. Discrepant scores between the two observers were averaged to arrive at a single final score. In order for a tumor core to be considered positive for Stat3 or Phospho-Stat3 (Tyr705) expression in either the cytoplasm or nucleus, it had to have a score of one (1) or greater from both observers.

Statistical Analysis. All analyses were completed using Statview 5.0.1 (SAS Institute Inc., Cary, NC). The correlation between the scores of both scorers and the relationships of Stat3 expression or Phospho-Stat3 (Tyr705) expression and clinicopathological parameters were measured using the χ^2 test. The prognostic significance of the parameters was assessed for pre-

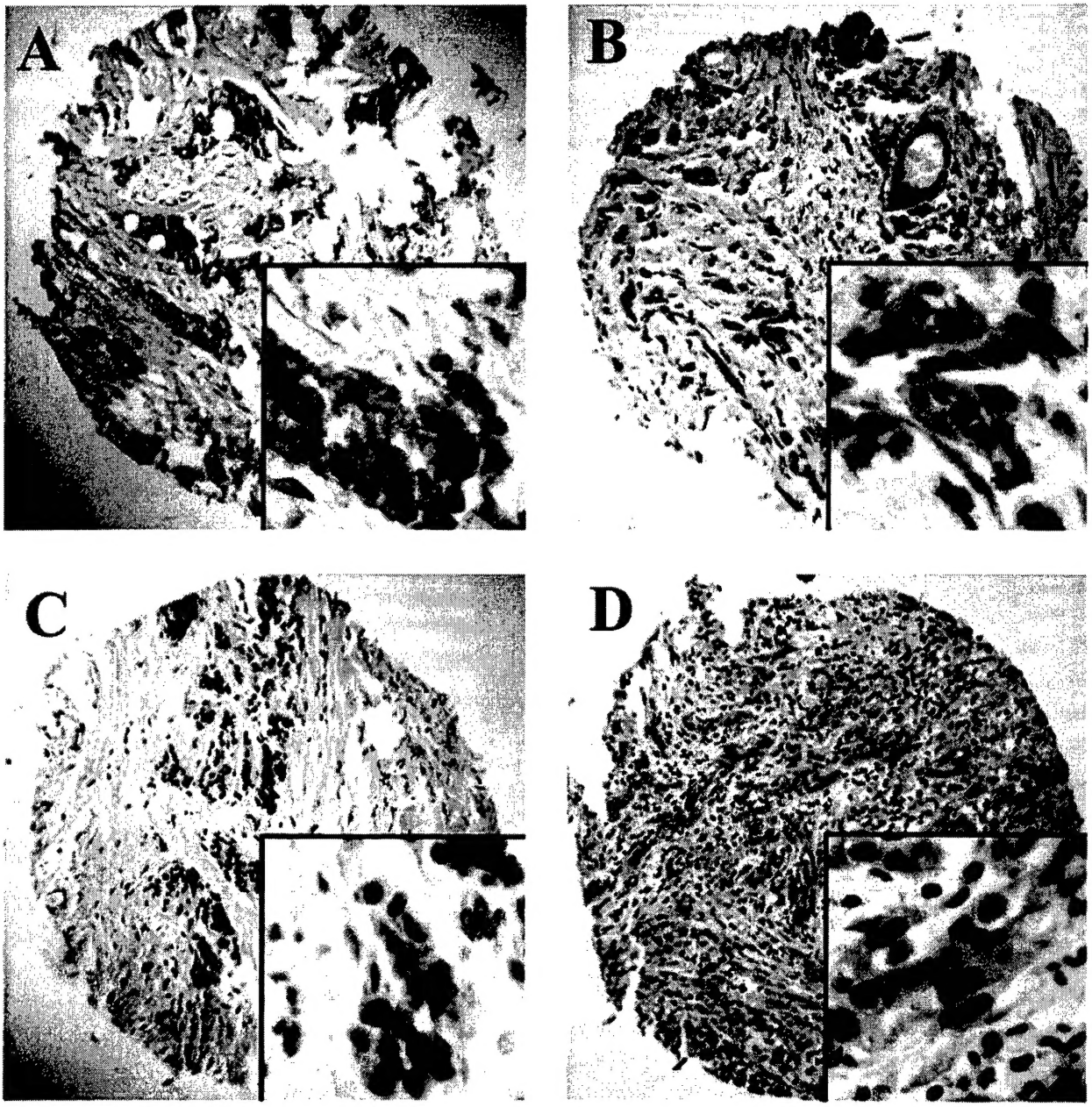

Fig. 1 Stat3 and Phospho-Stat3 (Tyr705) expression on representative node negative breast cancer tissue microarray spots as follows: *A*, strong Stat3 cytoplasmic staining; *B*, strong Stat3 nuclear staining shown with some cytoplasmic staining; *C*, strong Phospho-Stat3 (Tyr705) cytoplasmic staining; *D*, strong Phospho-Stat3 (Tyr705) nuclear staining. Figures are at ×100 magnification, inset at ×400 magnification.

dictive value using the Cox proportional hazards model with overall survival as an end point. Survival curves were calculated using the Kaplan-Meier method, with the significance evaluated using the Mantel-Cox long-rank test.

Results

Validation of the Antibodies on Archival Tissues. Because this study was done entirely using tissue microarrays with specimens from the 1960s to 1980s, immunohistochemical analysis of a validation tissue microarray was performed to study the preservation of antigenicity in older breast cancer tissue specimens. Although the validation was done for both the Stat3 antibody and the Phospho-Stat3 (Tyr705), we were particularly concerned that the phospho-specific antibody would be affected by long-term storage of the tissue in paraffin. Pathologist-based evaluation of the validation array showed representative staining patterns for both antibodies throughout the last 60 years. The number of patients sampled from each time period is insufficient

for statistical analysis, but no progressive or systematic loss of staining was seen for either antibody.

Immunohistochemical Staining of Node-negative Breast Cancer Tissue Microarray. Of the 346 node-negative breast cancer tumors on the tissue microarray, 286 tumor cores (82.7%) were interpretable for Stat3 staining, of which 258 of them (90.2%) had associated survival information. Uninterpretable spots were because of either loss of tissue on the tissue microarray or no tumor cells in the spot. The immunohistochemical staining of the breast cancer tissue microarray with Stat3 showed cytoplasmic (Fig. 1*A*) and/or nuclear (Fig. 1*B*) localization. There were 198 tumors (69.2%) that were positive for Stat3 cytoplasmic staining and 66 tumors (23.1%) positive for Stat3 nuclear staining. The distribution of Stat3 cytoplasmic staining levels and Stat3 nuclear staining levels are shown in Fig. 2, *A* and *B*, respectively. A subset of 64 tumors was positive for both Stat3 cytoplasmic staining and Stat3 nuclear staining (22.4%).

Staining with Phospho-Stat3 (Tyr705) also showed cytoplasmic (Fig. 1*C*) and/or nuclear localization (Fig. 1*D*). There were 285 tumor cores (82.4%) interpretable for Phosho-Stat3 (Tyr705) staining, of which 255 (89.5%) had associated survival information. Uninterpretable spots were because of either loss of tissue on the tissue microarray or no tumor cells in the spot. There were 56 tumors (19.6%) positive for Phospho-Stat3 (Tyr705) cytoplasmic staining and 124 tumors (43.5%) positive for Phospho-Stat3 (Tyr705) nuclear staining. A subset of tumors was positive for both Phospho-Stat3 (Tyr705) nuclear and cytoplasmic staining (44 of 285, 15.4%). The distribution of Phospho-Stat3 (Tyr705) cytoplasmic and nuclear staining are respectively shown in Fig. 2, *C* and *D*.

Survival Analyses. The expression of Stat3 and Phospho-Stat3 (Tyr705) as evaluated by immunohistochemical staining were correlated with overall survival of the patients at both 5- and 20-year follow-up times. To determine whether Stat3 or Phospho-Stat3 (Tyr705) expression level is correlated with outcome, Kaplan-Meier survival curves were generated for each antibody and subcellular localization. There was no significant difference in overall survival for cytoplasmic Stat3 staining at either 5 years (Fig. 3*A*) or 20 years (Fig. 3*E*) of follow-up or for Phospho-Stat3 (Tyr705) cytoplasmic staining at follow-up of 5 years (Fig. 3*C*) or 20 years (Fig. 3*G*). However, significant survival differences were seen with Stat3 and Phospho-Stat3 (Tyr705) nuclear staining.

Positive Stat3 nuclear staining was significantly correlated with better outcome at 5 years of follow-up ($P = 0.0332$; Fig. 3*B*) but was not correlated with survival long term at 20 years (Fig. 3*F*). A significant correlation between Phospho-Stat3 (Tyr705) positive nuclear staining and better outcome was seen at both 5 and 20 years of follow-up (Fig. 3*D*; $P = 0.0054$) and (Fig. 3*H*; $P = 0.0376$) respectively. Sixty-four of 66 tumors positive for Stat3 nuclear staining were also positive for Stat3 cytoplasmic staining (97%) and, therefore, had virtually identical survival outcomes as Stat3 nuclear staining alone (5-year follow-up, $P = 0.0375$; 20-year follow-up, $P = 0.2140$; survival curves not shown). There was no significant difference in survival between tumors positive for both PhosphoStat3 (Tyr705) nuclear and cytoplasmic staining at either a 5-year survival cutoff ($P = 0.1098$) or 20 years ($P = 0.0829$; survival curves not shown).

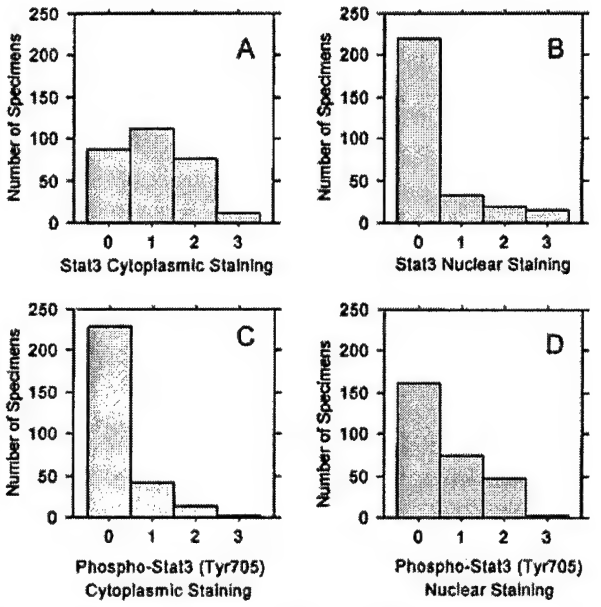

Fig. 2 Distribution of Stat3 and Phospho-Stat3 (Tyr705) immunohistochemical staining scores in node-negative breast cancer. *A*, Stat3 cytoplasmic staining scores; *B*, Stat3 nuclear staining scores; *C*, Phospho-Stat3 (Tyr705) cytoplasmic staining scores; *D*, Phospho-Stat3 (Tyr705) nuclear staining scores.

Clinicopathological Correlations and Multivariate Analyses. Multivariate analysis using the Cox proportional hazards model was done to assess the independent predictive value of Stat3 nuclear and Phospho-Stat3 (Tyr705) nuclear expression. The classic prognostic variables used to assess independence included tumor size, patient age at diagnosis, nuclear grade, Ki-67 nuclear staining as an index of proliferation rate, ER expression, PR expression, and HER2 expression. Stat3 nuclear staining was not a statistically significant independent predictor of overall survival ($P = 0.0556$; Table 1). However, Phospho-Stat3 (Tyr705) nuclear staining was independently predictive of overall survival ($P = 0.0469$) with a relative risk of 2.35 (Table 2). Tumor size of >2 cm was the only other variable with independent prognostic value in the multivariate analyses shown in Tables 1 and 2. Statistically significant variables in the multivariate analyses tables are highlighted in bold.

Discussion

To our knowledge, this is the first study to examine the expression of Stat3 and tyrosine phosphorylated Stat3 in breast cancer. We used standard immunohistochemical methods to assay activated Stat3 by both assessment of subcellular localization and phosphorylation status. Because activation of Stat3 signaling involves both tyrosine phosphorylation and translocation to the nucleus, we hypothesized that either or both of these parameters could provide a representation of tumors in which a Stat3-mediated signaling pathway had been activated. Our findings show activation of Stat3 signaling as assessed by either nuclear Stat3 or Phospho-Stat3 (Tyr705) is predictive of signif-

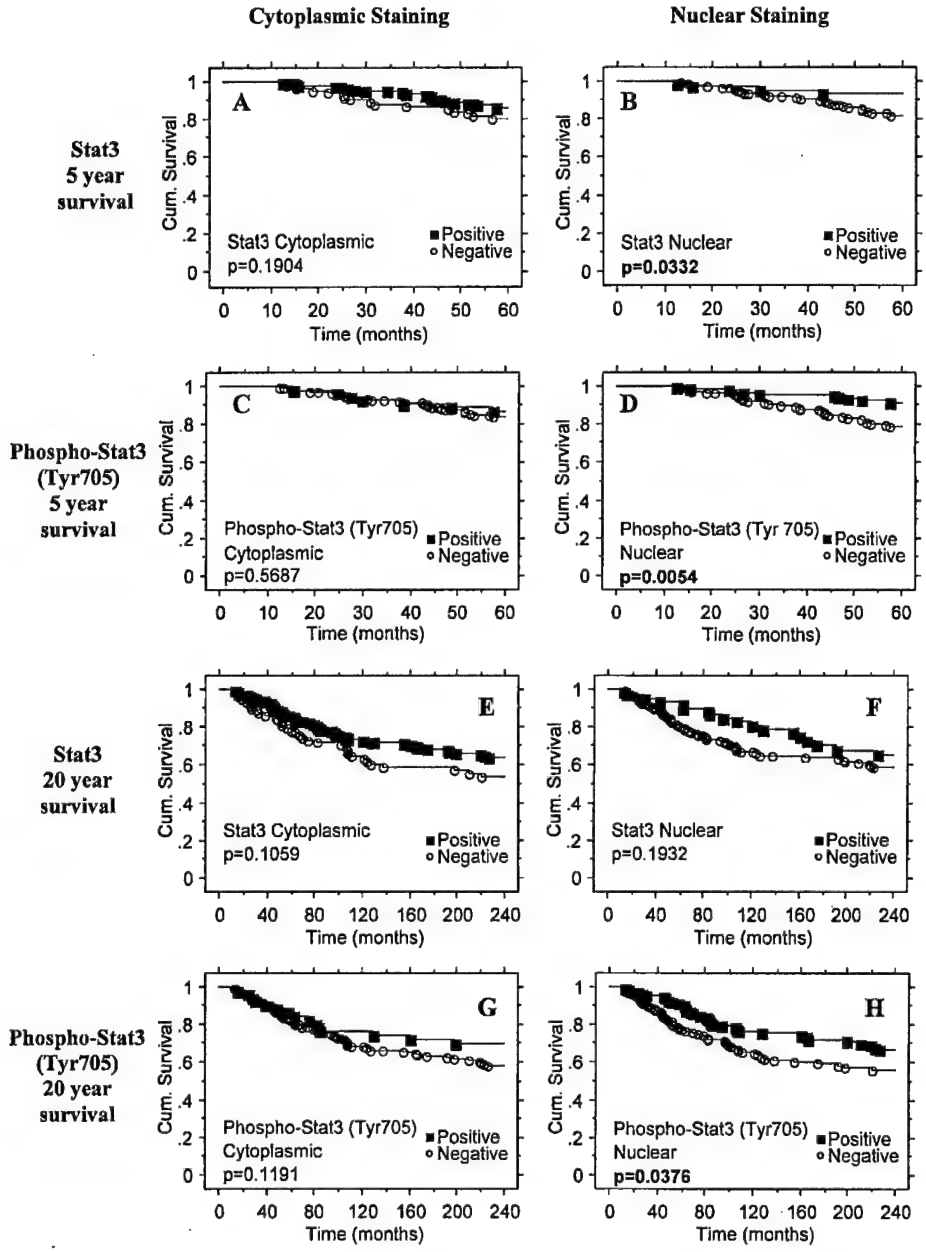

Fig. 3 Stat3 and Phospho-Stat3 (Tyr705) Kaplan-Meier survival curves in node-negative breast cancer. *A*, Stat3 cytoplasmic staining 5 year survival curve; *B*, Stat3 nuclear staining 5-year survival curve; *C*, Phospho-Stat3 (Tyr705) cytoplasmic staining 5-year survival curve; *D*, Phospho-Stat3 (Tyr705) nuclear staining 5-year survival curve; *E*, Stat3 cytoplasmic staining 20-year survival curve; *F*, Stat3 nuclear staining 20-year survival curve; *G*, Phospho-Stat3 (Tyr705) cytoplasmic staining 20-year survival curve; *H*, Phospho-Stat3 (Tyr705) nuclear staining 20-year survival curve.

icantly better clinical outcome. Furthermore, nuclear Phospho-Stat3 (Tyr705) is independent of all other commonly used prognostic markers and pathological parameters, except for tumor size.

The finding that activated Stat3 is associated with better outcome in breast cancer is subject to numerous interpretations. Because Stat3 is known to be persistently activated in src-transformed lines (25, 26), it is not surprising to find it activated in a large fraction of the tumors. The fact that it is associated with better outcome may simply mean that tumors that activate these pathways are less aggressive than tumors that progress even in the absence of Stat3 activation. Alternatively, it may be that Stat3 plays a role as a tumor suppressor protein. Evidence that Stat3 plays a role in cellular differentiation and apoptosis (8) may be consistent with better outcome in breast cancer if nuclear Phospho-Stat3 expression is selecting a group of well-differentiated tumors.

Constitutive Stat3 activation has been found in many types of cancers, including prostate (18), ovary (27), leukemia (28), and breast (16), however, there is very little data on its affect on outcome. We hope the availability of the Phospho-Stat3 antibody and our data will stimulate others to test for correlation with improved patient survival in other tumor types. Although additional investigation is needed to dissect

Table 1 Multivariate analysis of clinicopathological parameters and nuclear Stat3 expression

Multivariate analysis of Stat3 and prognostic factors with 5 year overall survival with 198 tumors (performed using a Cox proportional hazards model).

Variable	OS[a] *P*	Hazard ratio (95% CI)
Nuclear grade (high)	0.1958	2.25 (0.66–7.72)
Ki-67 (high)	0.4821	1.33 (0.60–2.93)
ER (neg)	0.9330	1.04 (0.44–2.45)
PR (neg)	0.4910	1.29 (0.62–2.70)
Her2 (pos)	0.9973	0.99 (0.38–2.55)
Age (young)	0.7682	0.81 (0.41–1.93)
Tumor size (>2 cm)	**0.0341**	**2.29 (1.06–4.93)**
Stat3 nuclear staining (neg)	0.0556	2.85 (0.97–8.33)

[a] OS, overall survival; CI, confidence interval; neg, negative; pos, positive.

Table 2 Multivariate analysis of clinicopathological parameters and nuclear Phospho-Stat3 (Tyr705) expression

Multivariate analysis of Phospho-Stat3 (Tyr705) and prognostic factors with 5-year overall survival with 195 tumors (performed using a Cox proportional hazards model).

Variable	OS *P*	Hazard ratio (95% CI)
Nuclear grade (high)	0.0674	3.96 (0.91–16.82)
Ki-67 (high)	0.5400	1.28 (0.56–2.78)
ER (neg)	0.6935	0.84 (0.35–2.03)
PR (neg)	0.7972	1.10 (0.53–2.30)
Her2 (pos)	0.8310	1.11 (0.43–2.84)
Age (young)	0.3764	1.42 (0.65–3.10)
Tumor size (>2 cm)	**0.0412**	**2.21 (1.03–4.74)**
Phospho-Stat3 (Tyr705) nuclear staining (neg)	**0.0469**	**2.35 (1.01–5.46)**

OS, overall survival; CI, confidence interval; neg, negative; pos, positive.

the different mechanisms of Stat3 signaling and its role in breast cancer development, many downstream targets have been identified, including cyclin D1, c-myc, p21 WAF1/CIP1, and Bcl-xL. The protein products of these targets are potential candidates for future investigations using our node-negative breast cancer cohort or other similar cohorts.

References

1. Darnell, J. E., Jr., Kerr, I. M., and Stark, G. R. Jak-STAT pathways and transcriptional activation in response to IFNs and other extracellular signaling proteins. Science (Wash. DC), *264:* 1415–1421, 1994.

2. Takeda, K., Noguchi, K., Shi, W., Tanaka, T., Matsumoto, M., Yoshida, N., Kishimoto, T., and Akira, S. Targeted disruption of the mouse Stat3 gene leads to early embryonic lethality. Proc. Natl. Acad. Sci. USA, *94:* 3801–3804, 1997.

3. Bromberg, J., and Darnell, J. E., Jr. The role of STATs in transcriptional control and their impact on cellular function. Oncogene, *19:* 2468–2473, 2000.

4. Guschin, D., Rogers, N., Briscoe, J., Witthuhn, B., Watling, D., Horn, F., Pellegrini, S., Yasukawa, K., Heinrich, P., Stark, G. R., *et al.* A major role for the protein tyrosine kinase JAK1 in the JAK/STAT signal transduction pathway in response to interleukin-6. EMBO J., *14:* 1421–1429, 1995.

5. Turkson, J., and Jove, R. STAT proteins: novel molecular targets for cancer drug discovery. Oncogene, *19:* 6613–6626, 2000.

6. Philp, J. A., Burdon, T. G., and Watson, C. J. Differential activation of STATs 3 and 5 during mammary gland development. FEBS Lett., *396:* 77–80, 1996.

7. Chapman, R. S., Lourenco, P., Tonner, E., Flint, D., Selbert, S., Takeda, K., Akira, S., Clarke, A. R., and Watson, C. J. The role of Stat3 in apoptosis and mammary gland involution. Conditional deletion of Stat3. Adv. Exp. Med. Biol., *480:* 129–138, 2000.

8. Chapman, R. S., Lourenco, P. C., Tonner, E., Flint, D. J., Selbert, S., Takeda, K., Akira, S., Clarke, A. R., and Watson, C. J. Suppression of epithelial apoptosis and delayed mammary gland involution in mice with a conditional knockout of Stat3. Genes Dev., *13:* 2604–2616, 1999.

9. Sartor, C. I., Dziubinski, M. L., Yu, C. L., Jove, R., and Ethier, S. P. Role of epidermal growth factor receptor and STAT-3 activation in autonomous proliferation of SUM-102PT human breast cancer cells. Cancer Res., *57:* 978–987, 1997.

10. Garcia, R., Bowman, T. L., Niu, G., Yu, H., Minton, S., Muro-Cacho, C. A., Cox, C. E., Falcone, R., Fairclough, R., Parsons, S., Laudano, A., Gazit, A., Levitzki, A., Kraker, A., and Jove, R. Constitutive activation of Stat3 by the Src and JAK tyrosine kinases participates in growth regulation of human breast carcinoma cells. Oncogene, *20:* 2499–2513, 2001.

11. Garcia, R., Yu, C. L., Hudnall, A., Catlett, R., Nelson, K. L., Smithgall, T., Fujita, D. J., Ethier, S. P., and Jove, R. Constitutive activation of Stat3 in fibroblasts transformed by diverse oncoproteins and in breast carcinoma cells. Cell Growth Differ., *8:* 1267–1276, 1997.

12. Page, C., Huang, M., Jin, X., Cho, K., Lilja, J., Reynolds, R. K., and Lin, J. Elevated phosphorylation of AKT and Stat3 in prostate, breast, and cervical cancer cells. Int. J. Oncol., *17:* 23–28, 2000.

13. Bromberg, J. Signal transducers and activators of transcription as regulators of growth, apoptosis and breast development. Breast Cancer Res., *2:* 86–90, 2000.

14. Watson, C. J., and Miller, W. R. Elevated levels of members of the STAT family of transcription factors in breast carcinoma nuclear extracts. Br. J. Cancer, *71:* 840–844, 1995.

15. Perou, C. M., Jeffrey, S. S., van de Rijn, M., Rees, C. A., Eisen, M. B., Ross, D. T., Pergamenschikov, A., Williams, C. F., Zhu, S. X., Lee, J. C., Lashkari, D., Shalon, D., Brown, P. O., and Botstein, D. Distinctive gene expression patterns in human mammary epithelial cells and breast cancers. Proc. Natl. Acad. Sci. USA, *96:* 9212–9217, 1999.

16. Berclaz, G., Altermatt, H. J., Rohrbach, V., Siragusa, A., Dreher, E., and Smith, P. D. EGFR dependent expression of Stat3 (but not STAT1) in breast cancer. Int. J. Oncol., *19:* 1155–1160, 2001.

17. Bartoli, M., Gu, X., Tsai, N. T., Venema, R. C., Brooks, S. E., Marrero, M. B., and Caldwell, R. B. Vascular endothelial growth factor activates STAT proteins in aortic endothelial cells. J. Biol. Chem., *275:* 33189–33192, 2000.

18. Campbell, C. L., Jiang, Z., Savarese, D. M., and Savarese, T. M. Increased expression of the interleukin-11 receptor and evidence of Stat3 activation in prostate carcinoma. Am. J. Pathol., *158:* 25–32, 2001.

19. Battifora, H. The multitumor (sausage) tissue block: novel method for immunohistochemical antibody testing. Lab. Investig., *55:* 244–248, 1986.

20. Kononen, J., Bubendorf, L., Kallioniemi, A., Barlund, M., Schraml, P., Leighton, S., Torhorst, J., Mihatsch, M. J., Sauter, G., and Kallioniemi, O. P. Tissue microarrays for high-throughput molecular profiling of tumor specimens. Nat. Med., *4:* 844–847, 1998.

21. Rimm, D., Camp, R., Charette, L., Costa, J., Olsen, D., and Reiss, M. Tissue microarray: a new technology for amplification of tissue resources. Cancer J., *7:* 24–31, 2001.

22. Camp, R. L., Charette, L. A., and Rimm, D. L. Validation of tissue microarray technology in breast carcinoma. Lab. Investig., *80:* 1943–1949, 2000.

23. Gillett, C. E., Springall, R. J., Barnes, D. M., and Hanby, A. M. Multiple tissue core arrays in histopathology research: a validation study. J. Pathol., *192:* 549–553, 2000.

24. Torhorst, J., Bucher, C., Kononen, J., Haas, P., Zuber, M., Kochli, O. R., Mross, F., Dieterich, H., Moch, H., Mihatsch, M., Kallioniemi, O. P., and Sauter, G. Tissue microarrays for rapid linking of molecular changes to clinical endpoints. Am. J. Pathol., *159:* 2249–2256, 2001.

25. Bromberg, J. F., Horvath, C. M., Besser, D., Lathem, W. W., and Darnell, J. E., Jr. Stat3 activation is required for cellular transformation by v-src. Mol. Cell. Biol., *18:* 2553–2558, 1998.

26. Turkson, J., Bowman, T., Garcia, R., Caldenhoven, E., De Groot, R. P., and Jove, R. Stat3 activation by Src induces specific gene regulation and is required for cell transformation. Mol. Cell. Biol., *18:* 2545–2552, 1998.

27. Huang, M., Page, C., Reynolds, R. K., and Lin, J. Constitutive activation of stat 3 oncogene product in human ovarian carcinoma cells. Gynecol. Oncol., *79:* 67–73, 2000.

28. Xia, Z., Sait, S. N., Baer, M. R., Barcos, M., Donohue, K. A., Lawrence, D., Ford, L. A., Block, A. M., Baumann, H., and Wetzler, M. Truncated STAT proteins are prevalent at relapse of acute myeloid leukemia. Leuk. Res., *25:* 473–482, 2001.

29. Dolled-Filhart, M., and Rimm, D. L. Tissue microarray technology: A new standard for molecular evaluation of tissue?, Principals and Practice of Oncology Updates. *16:* 1–11, 2002.

44

JAKS AND STATS AS BIOMARKERS OF DISEASE

Marisa Dolled-Filhart[1,2] and David L. Rimm[2]
Departments of [1]Genetics and [2]Pathology, Yale University School of Medicine, New Haven, CT 06520, USA.

Key words: tumors, prognostic markers, biomarkers, protein expression, survival analysis

1. INTRODUCTION

The assessment of protein expression as a mechanism to define the stage of a disease or to predict disease outcome is a common goal of many studies. Investigators often hope that assessment of the level of expression of a given protein will show activation of a given pathway and thus suggest that activation of that pathway is intimately associated with disease progression. Although only a handful of tumor biomarkers are routinely used in clinical practice today, that number is growing. New information and new biomarkers raise the possibility of more precise disease classification resulting in more accurate prediction of outcome. Furthermore, new bio-specific therapies are now being developed that specifically interrupt known pathways of tumorigenesis. Thus, for many drugs now in clinical trials, it is important to assess biomarker expression as a mechanism to determine the activation of a given pathway and thus the eligibility of a given patient for the new bio-

P.B.Sehgal., D.E.Levy and T.Hirano (eds.), Signal. Transducers and Activators of Transcription (STATs): Activation and Biology, 000-000.

specific therapy. The JAK and STAT pathways are well described pathways with significant roles in tumorigenesis, as discussed throughout this book. In this chapter, we review the data on the use of expression of JAK and STAT proteins as a mechanism to classify tumors and prognosticate outcome. At the time this chapter is being written, there are no published works with large cohorts of greater than 100 patients examining the predictive value of these proteins in association with a bio-specific therapy. However, several smaller studies have investigated the changes in STAT levels of cultured tumor specimens or in patient samples before and after treatment with Interferon-α (IFN-α), a therapeutic agent used for several types of human malignancies.

Over 60 studies have been done assessing the levels of JAK and STAT proteins in a wide variety of tumor types, some focused mainly on expression levels or binding activity in tumors and others as part of larger studies of JAK/STAT function or roles in biologic processes and pathways. Also mentioned briefly in this chapter are investigations that have identified JAKs and STATs in high-throughput analyses of cancer "profiles". In order to distill this information into a readable review, we have divided the studies by organ system and have included a summary of JAK/STAT levels in tumors compared to control specimens by major organ system/organ site in Table 1. The major groups included in this chapter are: 1. Nervous system tumors (brain and meningioma), 2. Breast cancer, 3. Gastrointestinal/digestive system tumors (carcinoid, colorectal, esophageal, hepatocellular, and pancreatic), 4. Gynecological tumors, 5. Head and neck tumors (nasopharyngeal and oral), 6. Skin tumors (melanoma and squamous cell carcinoma), 7. Urological tumors (prostate and renal) and 8. Hematologic cancers (lymphoma, myeloma and leukemia).

2. TUMORS OF THE NERVOUS SYSTEM

It is thought that brain tumors produce cytokines not expressed in normal brain tissue that may cause paracrine or autocrine-related effects. Therefore, determination of the levels of JAKs and STATs may further delineate the involvement of such autocrine or paracrine loops in tumors of the central nervous system. Studies to date have included analysis of levels of a variety JAKs and STATs in different brain tumor subtypes and meningiomas, but thus far only in small cohorts and without determination of their relationship to clinical information.

Table 1. Overall JAK/STAT activity, protein and RNA levels in tumors compared to control levels grouped by major organ site[1]

	Nervous System	Breast Cancer	GI/Dig. System	Gynec-ologic	Head & Neck	Skin Tumors	Urologic Cancer	Hematol. Cancers
Stat1	Equivalent (36)[2,3] Higher (17)[4]	Higher (124)	--	Higher (39)	Higher (26)	Lower (12)[5] Higher (40)[6]	Equivalent (42)	Higher (363)
Stat2	Equivalent[7] (17) Higher[6] (17)	--	--	--	Higher (26)	Lower (12)	Equivalent (42)	Lower (4)
Stat3	Higher (96)	Higher (422)	Higher (68)	--	Higher (109)	Lower (12)[7] Higher (10)[8]	Higher (210)	Higher (394)
Stat4	--	--	--	--	--	--	Higher (42)	--
Stat5	Higher (34)	Lower (50)[8]	--	--	Lower (26)[9]	--	Equivalent (42)	Lower (4) Higher (97)
Stat6	Higher (34)	--	--	--	--	--	Higher (42)	--
Jak1	Equivalent (17)[10] Higher (17)[6]	--	--	--	--	--	Higher (11)	--
Jak2	Higher (34)	--	--	--	--	--	--	--
Jak3	--	Higher (3)	--	--	--	--	--	--
Tyk2	--	--	Higher (12)	--	--	--	--	--

[1] References and content of controls are given within the text by organ system, subgroups within organ systems are combined where identical. tumor/normal. comparative levels were seen in the majority of samples; differences are noted by footnotes.

[2] Brain tumors, low grade gliomas had slightly higher levels

[3] (*n*) = combined total. number of tumor samples anal. yzed in multiple studies (or single studies when only one exists for a particular category)

[4] Meningiomas

[5] SCC

[6] Melanoma

[7] Brain tumors

[8] Stat5a

[9] Stat5b

[10] Higher in medulloblastoma subtype only

2.1 Brain Tumors

Comparisons between levels of JAKs and STATs in 17 brain tumor specimens (six subtypes) and control peritumoral specimens by western blotting by Cattaneo et al. (1) showed that Jak1 expression in medulloblastoma was about 23 times higher than control levels, while the remaining tumors had low levels comparable to control levels. Higher Jak2 levels were seen across all tumor histotypes than in the controls, but there was no correlation with proliferative activity or degree of anaplasia. The tumors also had elevated levels of Stat3, Stat5 and Stat6 compared to the controls, with the highest expression of Stat3 and Stat5 in medulloblastomas. Stat1 was uniformly expressed in both tumors and controls, with slightly higher levels in low grade gliomas. The average levels of tumor Stat2 were in the same range as the controls.

Glioblastoma multiforme (GM) tumors are very aggressive and often contain rearrangements, gain of function mutations, amplifications or other alterations that cause elevated expression levels or constitutive activation of epidermal growth factor receptor (EGFR); Stat3 is a downstream target of EGF. Activated Stat3 levels were higher in tumors (18/19) than normal human astrocytes, white matter or normal adjacent tumor tissue controls by electrophoretic mobility shift assay (EMSA) experiments conducted by Rahaman et al. (2). Stat1 was present only at low or undetectable amounts. GM samples examined by immunohistochemistry (IHC) for PhosphoStat3 (Tyr705) showed that all 6 tumor sections examined had strongly positive stained nuclei compared to minimal immunoreactivity in the controls. Schaefer et al. (3) found that Stat3α was constitutively activated in most high grade tumors (11/13), low grade tumors (9/16), and most medulloblastoma tumors (7/8) by EMSA and supershift analyses. All of the tumors had higher levels of Stat3α than the normal brain control samples. In addition, glioma and medulloblastoma tumors assessed by western blotting showed that the majority of tumors had significantly higher levels of PhosphoStat3 (Tyr705) than controls, but not PhosphoStat1 (Tyr701). PhosphoStat3 (Tyr705) expression examined by IHC in glioma tumor sections localized predominantly to tumor endothelial cells.

2.2 Meningioma

There is limited information about the active status of JAK/STAT signaling pathways in mengioma. STATs were known to be present at the RNA level in meningiomas based on a study by Schrell et al. (4) that showed the existence of Stat1, Stat3 and Stat5 mRNA in cerebral meningioma samples from 10 patients by RT-PCR. Magrassi et al. (5) assessed 17

meningioma tumors by western blotting and found that all samples had significantly higher levels of Jak1, Jak2 and all STATs than normal non-cancer dura samples. There were no detectable levels of Jak3 or Tyk2 in any of the samples. When divided by neuropathological criteria, there were significant expression differences between the subtypes for all Stats except for Stat2. Stat6 expression in transitional meningiomas was higher than in other subtypes. Activation of Stat1 and Stat3 in the same samples were determined by use of phosphotyrosine-specific antibodies in western blotting, which showed that Stat1 and Stat3 were activated in all samples which expressed Stat1 or Stat3, respectively. As there have not been other studies of JAKs or STATs to date in this type of cancer, the clinical importance of their expression in meningioma remains unknown.

3. BREAST CANCER

Several studies have addressed the binding activity levels or expression of Stat1, Stat3 and Stat5 in breast cancer tissues, but only a few have correlated their results with patient information. Additionally, JAKs and STATs have been identified in multiple high-throughput analyses of breast cancer profiles, as will be described below. While some analyses of STAT expression in tumors have included relevance to clinical parameters such as patient survival, lymph node status and recurrence, JAKs have not been investigated as thoroughly in breast cancer samples. Neither JAKs nor STATs have been evaluated with regard to their clinical importance in patient responses to treatment, which is an important next step in determining their value in patient treatment.

3.1 Activation and Expression in Breast Cancer

Nuclear extracts from 51 breast cancer samples were analyzed by Watson et al. (6) by EMSA for Stat1/Stat3 binding activity. The highest incidence of Stat binding activity was seen in the invasive carcinomas: 15/16 (94%) cases had increased binding activity ($p<0.01$) compared to 1/8 (12%) of in situ carcinomas, 1/15 (7%) of fibroadenomas, and low or undetectable amounts in benign and normal breast specimens (with the exception of lactating breast samples). EMSA analysis by Garcia et al. (7) of Stats 1 and 3 showed increased Stat DNA binding activity in nuclear extracts of 18 of 23 (78%) matched sets of primary breast tumor and adjacent non-tumor specimens, which was attributed to activation of both Stat1 and Stat3 by supershift analysis in the majority of tumors. Analysis of Stat1, Stat3 and Stat5 DNA binding activity and tyrosine phosphorylation was studied in 73

invasive breast carcinomas by Widschwendter et al. (8). The predominantly activated STATs are Stat1 and Stat3, as strong Stat5 binding activity was seen in only 1 of 63 tumors (1.6%). A wide range of PhosphoStat1 (Tyr701) levels were seen among the samples by Western blotting, which correlated highly with EMSA measurements (p=0.004). Comparison of Stat3 DNA binding activity and Stat3 (Tyr705) immunoblotting results also showed a strong correlation (p=0.001).

Analysis of 50 breast lesions including normal tissue, fibroademonas, ductal and lobular neoplasias and invasive carcinomas for Stat5a expression by IHC was conducted by Bratthauer et al. (9). Stat5a expression was seen in all normal and fibroadenoma samples, whereas most intraepithelial and invasive neoplasms did not express Stat5a, suggesting from this study a correlation between Stat5a absence and disease progression.

3.2 Associations with Prognosis in Breast Cancer

A Kaplan-Meier survival curve in the study described above by Widschwendter et al. (8) showed that high Stat1 activity by either EMSA (p=0.003) or immunoblotting (p=0.010) was associated with longer survival. Cox analysis showed that low Stat1 was associated with an elevated risk of death (3.77-fold higher) and recurrence (6.66-fold higher). High Stat1 activation is also correlated with a lower frequency of relapses and with lymph node status (p=0.008) as the majority of lymph node negative patients had high Stat1 activation. Stat3 and Stat5 activity or phosphorylation levels were not associated with any statistically significant prognostic value in the cohort.

Immunohistochemical investigation of Stat1 and Stat3 in 62 primary breast cancers (49 invasive ductal carcinomas, 8 invasive lobular carcinomas, 1 mucinous carcinoma, 1 medullary carcinoma, 3 ductal carcinoma in situ) by Berclaz et al. (10) demonstrated that Stat1 and Stat3 were expressed only in the nuclei or cytoplasm of breast epithelium and not in myoepithelial cells, fibroblasts, or adipose tissue. Breast carcinoma had statistically significant higher expression of nuclear Stat1 ($p<0.03$), cytoplasmic Stat1 ($p<0.005$), nuclear Stat3 ($p<0.0001$) and cytoplasmic Stat3 ($p<0.0001$) than the normal breast tissue. Stat3 nuclear positivity was strongly correlated with EGFR expression ($p<0.0001$) and Her2 expression ($p<0.0014$). Expression of Stat1 or Stat3 was not significantly associated with clinical outcome, tumor stage, grade or lymph node status in this cohort.

A study in our laboratory (Dolled-Filhart et al., 11) investigated Stat3 and PhosphoStat3 (Tyr705) expression by IHC in a large cohort of lymph node-negative invasive breast carcinoma samples using tissue microarrays (reviewed in Dolled-Filhart and Rimm, 12). Both cytoplasmic and nuclear

staining were seen, but there was no significant association between Stat3 or PhosphoStat3 (Tyr705) cytoplasmic staining and any clinicopathologic parameters. Positive nuclear Stat3 staining was seen in 66/286 cases (23.1%), and positive nuclear PhosphoStat3 (Tyr705) staining was seen in 124/285 cases (43.5%). Patients with positive Stat3 nuclear staining had a significantly improved short-term 5 year survival (p=0.0332), while those patients with positive PhosphoStat3 (Tyr705) nuclear staining had a significantly improved survival in both short-term 5-year survival (p= 0.0054) and long-term 20-year survival (p=0.0376). Positive PhosphoStat3 (Tyr705) nuclear expression was an independent prognostic marker of better overall survival (p=0.0469) in the node-negative breast cancer cohort by multivariate analysis.

3.3 JAKs/STATs Identified in Breast Cancer Profiling

cDNA microarray analysis of breast cancer samples by Sorlie et al. (13) identified Stat1 as part of their discriminator gene set. Stat1 was also identified in the microarray analyses of Perou et al. (14) as a component of a cluster of IFN-regulated genes, and found that tumor samples showed four patterns of Stat1 staining by IHC. Jak1 was identified by Meric et al. (15)as one of the tyrosine kinases (TKs) expressed in breast cancer cell lines by degenerate RT-PCR, and confirmed to be expressed in the tyrosine kinase profiles of invasive breast carcinoma samples. A display array analysis of microdissected late-stage malignant breast cancer biopsies by Mellick et al. (16) identified Stat3 expressed both in tumor and stroma sections. Jak3b, a splice variant of Jak3, was found to be highly expressed by Western blot analysis by Lai et al. (17) in 3 out of 5 primary tumors compared to their matched normal breast epithelium, at levels equivalent to that found in the BT-474 cell line (a known high expresser of Jak3b).

4. GASTROINTESTINAL/DIGESTIVE SYSTEM TUMORS

Data on the biomarker status of JAKs and STATs in carcinoid, colorectal, esophageal, hepatocellular and pancreatic tumors are beginning to emerge, with some limited findings of prognostic value from small cohort studies. Future investigations of their relationship to patient survival and analysis of response to therapy in larger cohorts will be useful in defining the role of the JAK/STAT signaling pathway in these types of cancer.

4.1 Carcinoid Tumors

Immunohistochemical analysis of Stat1 and Stat2 in midgut carcinoid tumors both before and after patient treatment with IFN-α was conducted by Zhou et al. (18) with 82 total specimens from 45 patients (33 pre-treatment, 45 during treatment). Stat1 and Stat2 staining were significantly stronger ($p=0.001$ and $p=0.002$, respectively) after IFN-α treatment. There was no correlation between Stat expression and IFN-α treatment time. Tumors staining with both Stat1 and Stat2 showed a significant positive correlation between Stat1 and Stat2 expression ($p=0.0001$). Both also had prognostic value in the cohort by Kaplan-Meier analysis, with high Stat1 expression ($p=0.002$) and high Stat2 expression ($p=0.022$) each associated with better survival. As this is the only study the expression of JAKs or STATs in carcinoid tumor samples, additional studies are needed to further evaluate the importance of this pathway with regard to patient treatment.

4.2 Colorectal Tumors

A study by Chen et al. (19) compared the TK profiles of differently staged colorectal carcinoma (normal colon mucosa, adenomatous polyp, primary carcinoma and hepatic metastasis) by an RT-PCR based approach. Using a degenerate primer of common motifs in the catalytic domains of nearly all TKs, Jak1 was expressed uniformly low in all four stages, Jak3 was expressed only in normal tissue, and Tyk2 expression was seen only in the polyp.

4.3 Esophageal Cancer

Tyk2 expression was discovered in an esophageal squamous cell carcinoma (SCC) cell line by Nemoto et al. (20) by a PCR-based cloning technique used to identify TKs. Northern blotting of 12 matched normal and esophageal SCC tissue samples showed a statistically significant 1.59-fold increase ($p<0.005$) of Tyk2 RNA expression in the carcinoma compared to normal tissues. However, there was no significant difference in increased TK mRNA expression level and degree of differentiation. In a study of cell lines derived from surgical specimens, Watanabe et al. (21) found that 19 EGF-Stat1 pathway negative cell lines had poor survival ($p=0.0175$) in Kaplan Meier survival analysis, compared to the 3 EGF-Stat1 pathway positive cell lines with a preserved growth arrest pathway. It will be interesting to learn of the relevance of Tyk2 protein levels and EGF/Stat1 status in large tumor sample cohorts.

4.4 Hepatocellular Carcinoma (HCC)

Evidence has suggested that JAK/STAT signaling cascades may contribute to malignant transformation of hepatocytes in hepatocellular carcinogenesis. A study of 15 primary HCCs, their pericarcinomatous regions and five hepatic metastases by Liu et al. (22) found that STAT binding activity was increased in peritumoral tissue compared to normal liver tissue, but not in tumors. A study by Feng et al. (23) of 55 matched HCC and pericarcinomatous tissue samples by IHC showed that nuclear PhosphoStat3 (Ser727) expression was seen in 74.5% of HCC samples in a clustered expression pattern, compared to 23.6% of pericarcinomatous samples with a scattered expression pattern. The HCC samples had a significantly higher positive rate ($p<0.01$) and higher expression intensity ($p<0.01$), but there was no correlation with degree of differentiation. PhosphoStat3 (Ser727) staining was significantly correlated with downstream Stat3 target expression including c-jun expression in pericarcinomatous samples, and both c-jun and c-fos in the HCC samples.

4.5 Pancreatic Cancer

Larger studies are needed to assess the relevance of Stat3, or other JAKs and STATs, on a protein level in pancreatic cancer. Three pancreatic tumor specimens and matched normal pancreatic tissue were examined by Wei et al. (24) as part of a larger study involving pancreatic cancer cell lines and expression of vascular endothelial growth factor (VEGF), which has been with progression of pancreatic cancer and elevated activation of Stat3. The pancreatic cancer tissue in this study had significantly higher levels of Stat3 activity than the normal tissue in the 3 matched sets that were tested. The Stat3 activity was correlated with VEGF mRNA expression by Northern blotting. PhosphoStat3 (Tyr705) IHC on 10 matched sets of pancreatic tumor and normal pancreatic tissue samples displayed negative or weak protein expression the normal tissue, while pancreatic tumor epithelial cells had strong PhosphoStat3 (Tyr705) staining that directly correlated with strong VEGF and CD34 staining.

5. GYNECOLOGICAL TUMORS

Only a few small studies of JAK/STAT levels in gynecological tumors have been published. Expression of PhosphoStat3 (Tyr705) was investigated by Savarese et al. (25) in 23 ovarian carcinomas by IHC, of which 17 (74%) had positive nuclear staining. Jak2, PhosphoJak2, Stat5 and

PhosphoStat5 were present in tumor cells and capillary endothelial cells in all 16 of the cultured female reproductive organ tumors studied by IHC by Yasuda et al. (26). Quantitative real-time RT-PCR analysis of 39 microdissected ovarian tumors of various subtypes by Hough et al. (27) revealed that 87% of tumors had at least 5-fold increased Stat1 expression, 74% had at least 10-fold increased Stat1 expression[11], and 10% had at least 100-fold increased Stat1 expression when compared to glyerceraldehyde-3-phosphate dehydrogenase (GAPDH, a housekeeping gene control). Stat1 expression was statistically significantly correlated with expression of several other genes including EpCAM/GA733-2, Kop, TIMP-3, FR1, SLPI, ApoE and ceruloplasmin. It is unclear how Stat1, Stat3, Stat5 or Jak2 expression are related to factors of clinical value such as survival time, metastatses or treatment response in patients with gynecologic tumors as studies thus far have looked only at relative RNA or protein levels.

6. HEAD AND NECK TUMORS

The only STAT investigated in oralcarcinoma is Stat3, which is thought to be an early event in tumorigenesis based on several studies analyzing the expression and activation of Stat3 in head and neck squamous cell carcinoma (HNSCC) progression. Nasopharyngeal carcinomas have not been frequently investigated for JAK/STAT protein levels compared to normal tissues, although studies show that they are expressed and differentially regulated at least at an RNA level in cancer.

6.1 Nasopharyngeal carcinoma

An immunohistochemical analysis of Stat1, Stat3, Stat4 and Stat5 in nasopharyngeal tumors by Chen et al. (28) showed a combination of cytoplasmic and nuclear staining for Stat1, Stat3 and Stat5, and only cytoplasmic staining for Stat4. Heterogeneity within the nasopharyngeal tissue was noted as there was a mixture of strongly staining positive nuclei adjacent to negative nuclei. Xie et al. (29) used a cDNA array to identify genes differentially expressed between nasopharyngeal carcinoma (26 samples) and normal nasopharyngeal tissues (9 samples). They found that Stat1 and Stat2 RNA levels were upregulated in nasopharyngeal carcinoma

[11] The specimens of different subtypes with at least 10-fold increased expression of Stat1 were: serous – 65% (23 samples), clear cell – 100% (6 samples), endometroid – 83% (6 samples), mucinous – 75% (4 samples).

and Stat5b RNA levels were downregulated. Semi-quantitative analysis of normal and cancer tissue with RT-PCR for Stat1 and Stat2 confirmed their results. Additional studies are needed to determine the usefulness of JAKs and STATs as biomarkers for nasopharyngeal carcinoma.

6.2 Oral Carcinoma

Rubin Grandis et al. (30) compared 19 matched HNSCC samples with their corresponding distant normal mucosa and normal non-cancer patient mucosa. EMSA analysis showed that STAT activation was 10.6-fold higher in tumors (p=0.012) and 8.8 fold higher in distant normalmucosa (p=0.018) than in normal non-cancer patient mucosa. Immunoblot analysis demonstrated that tumors had statistically significant increases in Stat3 protein compared to distant normal tissue (2.32-fold, p=0.006) and normal non-cancer patient mucosa (2.19-fold, p=0.021). IHC with PhosphoStat3 (Tyr705) localized to epithelial cells in tumors and distant normal mucosa, and to basalepithelial cells in normal non-cancer patient mucosa.

Tumor samples from 90 patients with HNSCC of various stages were studied by Nagpal et al. (31) for Stat3 RNA and protein expression levels. By RT-PCR analysis, Stat3 RNA expression was seen in HNSCC stages I, II and IV with reduced expression in stage III, and no expression in normal samples. All 16 normal and premalignant lesion tissue samples were negative for Stat3 protein expression by IHC (except for one premalignant lesion with intermediate cytoplasmic Stat3 staining), while 74/90 tumor samples (82.2%) stained positively. There was a gradual decrease in Stat3 accumulation with the progression of tumorigenesis when comparing T stages I/II versus stages III/IV (p=.033). High levels of activated Stat3 were seen by IHC with PhosphoStat3 (Tyr705) at all stages of HNSCC with both cytoplasmic and nuclear localization present. There was no significant correlation between Stat3 expression and any clinicopathologic parameters in this study.

Masuda et al. (32) examined the relationship between PhosphoStat3 (Tyr705), cyclinD1 (a downstream target of Stat3), and clinicopathological parameters in a cohort of 51 primary tongue SCCs. Positive PhosphoStat3 (Tyr705) staining was seen in 37% (7/19 cases) of tumors, which was highly correlated with positive cyclinD1 expression (p<0.001), nodal metastases (p=0.016) and clinical stage (p=0.03). Kaplan-Meier survival curves showed that patients with positive PhosphoStat3 (Tyr705) staining had statistically significant lower disease-specific survival rates than those with negative staining (p<0.01). This is the opposite result from that seen in breast cancer, but this study has a relatively small cohort.

7. SKIN TUMORS

Studies have thus far have only analyzed levels of some STATs in melanoma and skin squamous cell carcinomas in small cohorts. High levels of IFN-α treatment for 1 year has been demonstrated to be beneficial with regard to relapse-free and overall survival for patients with resected high-risk early cutaneous melanoma(33, 34). Interesting work has begun to emerge about the effect of IFN-α treatment on levels of STAT proteins.

7.1 Melanoma

EMSA analysis by Niu et al. (35) of normal skin specimens and 10 melanoma specimens showed that many tumor tissues had elevated STAT DNA binding activity compared to little or no STAT binding activity seen in the normal skin samples. By competition and supershift EMSA analysis, they found that Stat3 homodimers and Stat3:Stat1 heterodimers were activated in the primary tumor tissues. Chawla-Sarkar et al. (36) found that 27 of 30 melanoma biopsy samples (90%) had high Stat1 levels compared to cell line controls by immunoblotting. Immunohistochemical evaluation of Stat1 in 24 of the biopsies showed varying levels of cytoplasmic Stat1 in the tumors as well as in the normal cells.

Two studies have evaluated the response of cultured melanoma samples to IFN-α treatment. Carson et al. (37) found that cultured malignant melanoma tumors of 17 patients showed dose-dependent Stat1 activation after treatment with IFN-α. Kirkwood et al. (38) studied the resected precursor lesions of 5 patients with a history of melanoma before and after the patients were treated with 3 months of low levels of subcutaneous IFN-α injections. The four most atypical nevi of each patient were photographed and marked; two were removed, while the other two were removed only after IFN-α treatment. Stat1, Stat2 and Stat3 IHC staining were analyzed microscopically by spectral imaging due to the difficulties of accurately assessing subcellular localization and intensity in pigmented melanoma lesions. Cytoplasmic and nuclear staining were seen for both Stat1 and Stat3 in the basal layer keratinocyes and junctional melanocytes, with Stat3 expressed in the upper epidermis as well. Stat2 expression was almost completely cytoplasmic in both treated and untreated nevi. EMSA and supershift analysis identified Stat1 and Stat3 homodimers/heterodimers as being activated in the untreated lesions. Examination by immunoblotting with a PhosphoStat3(Tyr705) antibody demonstrated that Stat3 was dephosphorylated in response to IFN-α treatment.

7.2 Squamous cell carcinoma (SCC)

Examination of 16 aggressive skin SCC specimens and matched adjacent non-cancer tissue from 12 patients were examined by IHC for Stat1a/b, Stat2, Stat3a and Stat3b by Clifford et al. (39). In the majority of samples, STAT protein expression was reduced in tumors compared to the adjacent non-malignant epidermal cells. Lower expression in the tumor compared to the adjacent non-cancer epithelial cells were seen in the following percentage of cases (ranging from 12-16 tumor samples): Stat1a/b (69%), Stat2 (67%), Stat3a (83%), Stat3b (67%). Stat3a and Stat3b highly stained basal cells in the adjacent non-cancer epithelium. Quantitative measurements of antibody staining by densitometry showed statistically significant decreases ($p<0.05$) in tumor expression of Stats in some matched specimens.

8. UROLOGICAL TUMORS

Several investigations of Stat1, Stat3 and Stat5 in prostate cancer have compared expression levels with controls and have looked for associations with different stages of progression. However, the prognostic value of these levels remain to be determined. Studies of the expression of JAKs in prostate cancer, and of JAKs and STATs in renal cell carcinoma, are very limited.

8.1 Prostate Cancer

Stat3 is the most often studied JAK/STAT in prostate cancer tumor samples for activation, protein expression and associations with progression, Gleason scores or prostate specific antigen (PSA) levels. Although all STATs have been examined in at least one prostate cancer cohort, information about JAK remains unstudied aside from identification in a TK profiling study.

8.1.1 Activation and Expression in Prostate Cancer and Associations with Cancer Progression

EMSA analysis by Mora et al. (40) of 45 matched primary prostate tumors and adjacent nontumor prostate tissue showed that 37 tumor cases (82%) had elevated Stat3 DNA binding activity. Immunohistochemical analysis of PhosphoStat3 (Tyr705) in these same matched samples showed nuclear staining of tumor epithelial cells and low nuclear staining levels in normal adjacent tissue basal epithelial cells. PhosphoStat3 (Tyr705) levels were significantly higher in malignant specimens compared to non-tumor

specimens ($p<0.001$) and were correlated with Gleason scores >=7 ($p<.0007$), but not with initial serum PSA levels or clinical stage. Dhir et al. (41) compared Stat3 activity levels in 42 matched primary prostate tumors and adjacent normal tissue, and 20 normal prostates by EMSA. Stat3 activity was higher in tumor samples than the matched adjacent tissue in 18 cases (43%), had comparable levels in 10 cases (24%), and had lower levels in 14 cases (33%). There was no statistically significant difference in Stat3 activity between the matched tumor and adjacent normal samples, but Stat3 levels were increased significantly ($p<0.01$) in the tumor and adjacent tumors samples compared to the organ donor normal prostate tissue. Immunohistochemical analysis of PhosphoStat3 (Tyr705) showed moderate or strong expression in foci of adenocarcinoma and normal adjacent tissue and weak or negative staining in the normal donor prostate tissues. Elevated PhosphoStat3 (Tyr705) nuclear staining was seen in the tumor specimens compared to the adjacent normal tissues ($p<0.0001$), which correlated with the EMSA Stat3 activity results.

Campbell et al. (42) examined PhosphoStat3 (Tyr705) expression in 21 prostate carcinomas and 28 normal or benign prostatic hyperplasic (BPH) by IHC. Nuclear staining was seen in malignant and nonmalignant glandular epithelial cells, but was weaker in the nonmalignant samples. A high frequency of strong PhosphoStat3 (Tyr705) nuclear staining was seen in 15/21 tumor samples (71%) compared only 2/28 normal or BPH samples (7.1%). The difference between malignant and non-malignant samples was statistically significant ($p=0.0001$). Similarly, an assessment of PhosphoStat3 (Tyr705) by IHC by Giri et al. (43) on 12 prostate cancer specimens from radical prostatectomies showed positive nuclear staining in the prostate cancer epithelial cells in 10/12 cases (83%).

EMSA analysis of STATs in prostate cancer by Ni et al. (44) showed that Stat6 activity was higher in the tumor samples than the matched adjacent tissue in 28/42 cases (67%). There was a statistically significant higher levels of Stat6 in the tumor samples than the matched normal tissue levels ($p<.05$) or normal donor prostate levels ($p<.01$), but with no correlation to pretreatment PSA or Gleason grade. Stat4 activity was higher in the tumor samples than the matched adjacent tissue in 18 cases (43%), had comparable levels in 11 cases (26%), and lower levels in 13 cases (31%), but with no significant difference between prostate tumors and their matched normal adjacent tissue or normal donor tissue. Negligible levels of active Stat1, Stat2 or Stat5 were found in prostate tumor samples.

8.1.2 JAKs/STATs Identified in Prostate Cancer Profiling

Jak1 and Jak2 were identified by degenerate RT-PCR analyses of TKs expressed in prostate cancer bone marrow metastases from 6 patients by

Chott et al. (45). Metastatic prostate cancer expression of Jak1 was analyzed by IHC, whereby weak to moderate expression was seen in the tumor cells of all 8 bone marrow biopsies studied. Jak1 expression was weak in normal prostate luminal epithelial cells, but seen with uniform moderate to strong staining in 3 primary prostate cancers. Jak1 expression was increased in primary and metastatic tumor cells compared to normal prostate tissue.

8.2 Renal Cell Carcinoma (RCC)

The only study found by the authors to date determining protein expression levels of JAKs or STATs in RCC is by Horiguchi et al. (46). They compared the expression levels, incidence and prognostic associations of Stat3 and PhosphoStat3 (Tyr705) in 48 matched sets of matched archival RCC adjacent non-neoplastic kidney tissue samples. Stat3 IHC in tumor samples demonstrated both cytoplasmic and nuclear staining, while predominantly nuclear staining was seen in tumors with PhosphoStat3 (Tyr705) staining. Adjacent non-neoplastic kidney tissue stained weakly with Stat3 and PhosphoStat3 (Tyr705). High levels of PhosphoStat3 (Tyr705) were seen in 24/48 (50%) RCC samples, which correlated with metastasis (p=0.0094). Tumors with high levels of Phospho-Stat3 (Tyr705) were significantly associated (p=0.0117) with shorter disease-specific survival by Kaplan Meier analysis; high PhosphoStat3 (Tyr705) staining was an independent prognostic marker in multivariate analysis (p=0.0439). The Stat3 and PhosphoStat3 (Tyr705) levels were independent of each other, suggesting from this cohort that Stat3 activation in RCC was due to increased Tyr705 phosphorylation rather than Stat3 overexpression.

9. HEMATALOGIC CANCER

While many studies have investigated STATs in lymphoma, myeloma and leukemia, only a few studies have correlated expression or activity with patient outcome or treatment response. Future investigations of the value of JAKs and STATs in predicting prognosis and therapeutic response will be of great interest in the treatment of hematologic cancers.

9.1 Hodgkins lymphoma (HL)

IHC analysis of nuclear Stat1 and nuclear Stat3 expression on a tissue microarray containing 288 HL biopsies by Garcia et al. (47) found that there were 236/267 cases positive for Stat1 (88.4%) and 145/261 cases (55.6%) positive for Stat3 in the Hodgkin and Reed-Sternberg (HRS) cells.

Comparisons with the 27 other markers investigated in the HRS cells on this cohort by IHC or ISH showed statistically significant direct relationships between Stat1 and Bax, CDK1, CDK2, Epstein-Barr Virus (EBV), Mib1 (Ki-67), NF-κB, Stat3 and TUNEL. Stat3 expression was directly correlated with EBV, Mib1 and Stat1. Survival analysis of classical HL cases using Kaplan-Meier curves and Cox regression showed a trend for association of high nuclear Stat3 expression and shorter survival, although it was not statistically significant (p=0.06). Analysis of HL samples by Chen et al. (28) found that nuclear Stat3 staining was seen in both EBV positive and EBV negative malignant HRS cells. Stat1 IHC showed low levels of nuclear staining in the EBV negative sample, but only cytoplasmic staining in the EBV positive tissue.

Stat5a expression by IHC was investigated by Hinz et al. (48) after Stat5a was found to be expressed at high levels in HRS cell lines compared to non-HRS cells in microarray analyses looking for target genes of NF-κB. Analysis of 24 classical HL cases by IHC showed that high cytoplasmic and nuclear staining was seen in over 80% of the HRS cells in the lymph node sections compared to adjacent benign cells. Stat5a staining was weaker in lymphocyte predominance Hodgkins disease malignant and histocytic cells (only 4 of 14 cases positive for Stat5 nuclear staining) compared to classical HL.

9.2 Non-Hodgkins lymphoma (NHL)

A set of 149 NHL cases were examined for Stat3 expression by Zamo et al. (49), which included 64 anaplastic large cell lymphoma (ALCL) cases, of which 21 were anaplastic lymphoma kinase positive (ALK+) cases and 43 cases were ALK negative (ALK-). Immunoblotting with PhosphoStat3 showed that the ALK+, but not ALK-, tumors showed detectable levels of PhosphoStat3. IHC analysis of Stat3 showed that 20/21 ALK+ tumors (95%) had nuclear Stat3 tumor cell staining, while only 1/43 ALK- tumors (2%) had nuclear Stat3 staining and the rest had cytoplasmic Stat3 staining. Other types of ALK- NHL were examined for Stat3 by IHC and only 4/85 cases (5%) exhibited positive nuclear Stat3 staining, suggesting that Stat3 activation is largely correlated with expression of ALK in NHL.

Examination of cutaneous T-cell lymphoma patients' skin lesions by Qin et al. (50) showed that all 6 mycosis fungoides samples and all 6 Sezary syndrome lesions had cytoplasmic Stat1, Stat2, Stat3 and Stat6 staining of malignant T cells by IHC. Some of the samples also had strong nuclear staining, and all had nuclear Stat5 staining, but without any significant correlation to disease progression. Peripheral blood mononuclear cells of 14 Sezary syndrome patients analyzed by Zhang et al. (51) showed that 9/14

(64%) had strong basal phosphorylated Jak3. Those same cases were also all positive for Stat5 phosphorylation, and 4 were positive for Stat3 phosphorylation (2 weak, 2 strong). Amplification of Jak2 was detected by comparative genomic amplification of 16 aggressive B-cell NHL cases in a study by Wessendorf et al. (52).

Microarray analysis comparisons between 9 common mantle cell lymphoma samples and 9 blastoid variant samples showed more frequent upregulation of several Stat3 downstream signaling targets (c-myc, Bcl-2 and pim-1) in the blastoid variants than in the mantle cell lymphomas (53). In another study of mantle cell lymphomas, Lai et al. (54) found that all 8 mantle-cell tumors investigated (7 small cell type, 1 blastoid variant) expressed PhosphoStat3 (Tyr705) and variable levels of PhosphoStat3 (Ser727) by blotting. Immunofluorescence with PhosphoStat3 (Tyr705) and PhosphoStat3 (Ser727) on four additional tumors showed nuclear expression, while Stat3 expression was predominantly cytoplasmic. The cases had more nuclei positive for PhosphoStat3 (Tyr705) than PhosphoStat3 (Ser272).

9.3 Phosphorylated STAT expression in HL and NHL

PhosphoStat3 (Tyr705), PhosphoStat5 (Tyr694) and PhosphoStat6 (Tyr641) expression was studied by Skinnider et al. (55) by IHC in both HL and NHL cases, including many subtypes[12]. Positive nuclear PhosphoStat3 (Tyr705) expression was seen in a significant number of cells in the reactive infiltrate and in HRS cells in 27/31 classical HL cases (87%), but with no significant difference according to subtype. Positive nuclear PhosphoStat3 (Tyr705) staining was not specific for classical HL as it was also seen in non-classical HL including NLPHL (50%), DLBCL (38%), TCRBCL (60%), ALCL (83%), and PTCL (60%).

Positive PhosphoStat5 (Tyr694) nuclear staining was observed in only 8/31 classical HL cases (26%), but was not seen in LDHL, NLPHL, DLBCL, TCRBL, and PTCL cases. Among ALCL cases, 3/6 (50%) were had positively stained nuclei.

Positive nuclear PhosphoStat6 (Tyr641) staining occurred in HRS cells in 25/32 classical HL samples (78%), with differential expression according to subtype. NSHL cases had significantly higher rates of positive expression than MCHL or LDHL cases. Positive nuclear expression was

[12] AL. CL = anaplastic large cell lymphoma with a T/null cell phenotype (6 cases), classical. HL (32 cases), DLBCL = diffuse large B-cell lymphoma (8 cases), LDHL = lymphocyte-depletion HL (3 cases), MCHL = mixed cell HL (8 cases), NLPHL = nodular lymphocyte predominance HL (4 cases), NSHL = nodular sclerosis HL (21 cases), PTCL = unspecified peripheral. T-cell lymphoma (5 cases), and TCRBCL = T-cell-rich B-cell lymphoma (5 cases)

significantly associated with IL-13 expression as determined by ISH analysis. PhosphoStat6 (Tyr641) nuclear staining was also seen in TCRBCL and ALCL cases, but not in NLPHL, DLBCL or PTCL cases. There was no correlation between EBV LMP-1 expression and PhosphoStat3 (Tyr705), PhosphoStat5 (Tyr694) or PhosphoStat6 (Tyr641) expression in HRS cells of classical HL cases.

9.4 Myeloma

STAT activity was evaluated in the mononuclear fraction of 24 multiple myeloma patient bone marrow specimens by Catlett-Falcone et al. (56). EMSA analysis showed that a third of patients had high elevation in activated STAT levels, compared to normal bone marrow samples which had little or no STAT activation. Supershift analysis revealed that Stat3 homodimers and Stat1:Stat3 heterodimers were the predominant activated STAT species, with a low frequency of Stat1 homodimers and no Stat5 activation seen in the samples.

9.5 Leukemia

The role of STAT activation in leukemogenesis has been studied because many cytokines involved in the proliferation and survival of hematopoetic cells cause activation of STAT signaling. Amongst the several types of leukemia samples examined in the studies below, it appears that Stat1, Stat3 and Stat5 are activated in acute leukemia. Studies thus far have primarily focused on acute myelogenous leukemia and suggest that STAT activity is linked with poorer prognosis.

9.5.1 Acute Myelogenous Leukemia

Acute myelogenous leukemia (AML) is characterized by clones of malignant myeloid cells that results in aberrant production of hematopoietic cells. In a study of bone marrow cells from 63 AML patients with associated treatment information and follow-up time of 4 years, Benekli et al. (57) examined the pre-treatment levels of Stat3α and Stat3β by immunoblotting and Stat3 activity levels by EMSA. There was no significant association between Stat3 isoform expressed and Stat3 activation status. Stat3 activity was seen in 28/63 patients (44%) but no activity was present in the monocytes or granulocytes from 3 normal donor blood samples. Stat5 activity was seen in 11/50 patients (22%). Stat3 activity showed significantly shorter disease-free survival by univariate analysis ($p=0.01$) and Kaplan Meier curves than

patients without Stat3 activity; the subset with Stat3β expression had a significantly shorter disease free survival time (p=0.006) than the remaining patients. The bone marrow aspirates or peripheral blood from 24 AML patients were examined by Biethahn et al. (58) and showed that 9/24 patients were completely deficient in at least one of the 4 JAK proteins. Stat1α, Stat1β, Stat3α and Stat3β proteins were seen in all 24 patients, with the α isoform having higher levels than the β isoform. Stat5 protein was present in 21/24 (88%) patient samples.

Varying frequencies of AML patient samples with STAT activation and expression have been reported. Hayakawa et al. (59) studied STAT tyrosine phosphorylation status of AML samples and found that Stat3 phosphorylation occurred in 17/23 AML cases (74%) and Stat5 tyrosine phosphorylation occurred in 40/50 cases (80%). Stat3 activation and Stat5 activation occurred together in about 70% of samples and were correlated (p=0.04). Stat5 phosphorylation status was correlated with EMSA analysis, and there was no phosphorylated Stat5 in normal bone marrow cells. Stat5 isoform phosphorylation levels were further studied in a subset of 20 samples which showed that 15/20 (75%) expressed phosphorylated Stat5a and 18/20 (90%) expressed phosphorylated Stat5b. 20 pretreatment AML patients' peripheral blood cell blasts examined by Schuringa et al. (60) showed that 25% of samples had activated (phosphorylated) Stat3 by western blotting for both PhosphoStat3 (Tyr705) and PhosphoStat3(Ser727).

Gouilleux-Gruart (61) assessed the activation status of samples from 5 AML patients for several STATs. Stat1 was activated in 1/4 samples, Stat3 was activated in 5/5 samples, and Stat5 was activated in 2/5 samples, compared to no activation in normal control samples. Analysis of AML samples by Testa et al. (62) by EMSA determined that 2/15 samples (13%) had activated Stat5, which was confirmed by western blotting for Phospho-tyrosine Stat5. Weber-Nordt et al. (63) found activation of Stat1 and Stat3 in 10/14 AML samples but no activation in normal mononuclear cells. AML samples examined by Frank et al. (64) for tyrosine and serine phosphorylation status of Stat1 and Stat3 showed that Stat1 (8/26 tyrosine, 5/10 serine) and Stat3 (3/16 tyrosine, 5/10 serine) phosphorylation was present in samples. Normal B lymphocytes or tonsil CD5+ B cells did not have phosphorylation.

Xia et al. (65) analyzed 36 newly diagnosed AML pretreatment bone marrow samples by EMSA and found that 10/36 (28%) had activated Stat3, 8/36 (22%) had activated Stat5, and 0/10 samples had activated Stat6. In 27 samples analyzed for isoforms, 21/27 samples (79%) express the β isoforms. This study was followed up with analysis by the same group of the relationship between STAT activation and relapse with 17 additional patients(65). Stat3 activation was detected in 13/17 (76%) of AML samples at diagnosis and 4/17 (24%) upon relapse. Stat5 activation was detected in 3/17

samples (18%) a diagnosis and only 2/17 (12%) at relapse. There were 12/17 pretreatment samples (71%) expressing Statβ isoforms and 16/17 (94%) expressing it at relapse. However, there was no significant correlation of STAT activity or isoform expressed with duration of remission or karyotypic changes upon relapse.

9.5.2 Acute Lymphoblastic Leukemia

Only two studies so far have assessed STAT levels in acute lymphoblastic leukemia (ALL). Weber-Nordt et al. (63) observed Stat5 activation in 3/5 T-ALL (60%) and in 12/19 B-ALL samples (63%), but no activation in normal mononuclear cells. Gouilleux-Gruart (61) assessed the activation status of 2 ALL samples, and found 1/3 patients (33%) had activated Stat1, and 3/3 patients (100%) had activated Stat5, compared to no activation in normal control samples. B-ALL samples examined by Frank et al. (64) for Stat1 and Stat3 tyrosine and serine phosphorylation status showed phosphorylation of Stat1 (6/10 tyrosine, 5/10 serine) and Stat3 (9/10 tyrosine, 5/10 serine). Some T-ALL samples were also phosphorylated for Stat1 (6/10 tyrosine, 2/10 serine) and Stat3 (2/10 tyrosine, 4/10 serine).

9.5.3 Chronic Myelogenous Leukemia

The hallmark of chronic myelogenous leukemia (CML) is a translocation between chromosome 9 and chromosome 22 (Philadelphia chromosome translocation) that results in activation of the BCR/abl fusion gene, which may directly activate STAT signaling (66). Landolfo et al. (67) found that Stat1 was activated either constitutively or after in vitro IFN-α stimulation in 6/9 CML samples which were the complete responders. None of the IFN-α resistant cases expressed Stat1 suggesting that Stat1 shows a predictive correlation resistance of response to IFN-α in vitro in this small cohort. Analysis of 4 CML samples by Bruchova et al. (68) using cDNA microarrays did not find overexpression of STATs, but rather, transcriptional downregulation of Stat2 and Stat5 compared to controls. It will be interesting to determine the protein levels of STATs in a larger cohort to see if they are overexpressed as suggested by activation of BCR/abl, or downregulated.

9.5.4 Chronic Lymphoblastic Leukemia

Chronic lymphoblastic leukemia (CLL) is characterized by clonal expansion of B-lymphocytes that express CD5 and slowly accumulate. Investigation of 13 CLL lymphocyte samples by Frank et al. (64) demonstrated that Stat1 (0/13 tyrosine, 32/32 serine) phosphorylation levels and Stat3 (0/13 tyrosine, 32/32 serine) phosphorylation levels were

significantly different ($p<0.001$) compared to other leukemias; normal B lymphocytes or tonsil CD5+ B cells did not have phosphorylation. CLL was the only type with consistent serine phosphorylation.

B-cell chronic lymphoid leukemia (B-CLL) is highly heterogeneous and usually sensitive to DNA damage, and responding by undergoing apoptotic death. However, there is a clinically distinct subset of B-CLL that is resistant to in vitro apoptotic induction. Microarray analysis by Vallat et al. (69) found that Stat1 was one of the genes that was constitutively downregulated in the 4 BCLL resistant samples compared to the 3 sensitive samples. Their results were verified in 15 additional samples (7 sensitive, 8 resistant) by RT-PCR.

ACKNOWLEDGEMENTS

This work was supported by the US Army Department of Defense Breast Cancer Research Program grants DAMD17-03-1-0349 (MDF) and DAMD 17-01-1-0463 (DLR), the Patrick and Catherine Weldon Donaghue Foundation for Medical Research (DLR), and NIH grants K0-8 ES11571 and RO-1 GM57604 NCI (DLR).

REFERENCES

1. Cattaneo, E., Magrassi, L., De-Fraja, C., Conti, L., Di Gennaro, I., Butti, G., and Govoni, S. (1998) *Anticancer Research* **18**, 2381-2387
2. Rahaman, S. O., Harbor, P. C., Chernova, O., Barnett, G. H., Vogelbaum, M. A., and Haque, S. J. (2002) *Oncogene* **21**, 8404-8413
3. Schaefer, L. K., Ren, Z., Fuller, G. N., and Schaefer, T. S. (2002) *Oncogene* **21**, 2058-2065
4. Schrell, U. M., Koch, H. U., Marschalek, R., Schrauzer, T., Anders, M., Adams, E., and Fahlbusch, R. (1998) *J Neurosurg* **88**, 541-548
5. Magrassi, L., De-Fraja, C., Conti, L., Butti, G., Infuso, L., Govoni, S., and Cattaneo, E. (1999) *J Neurosurg* **91**, 440-446
6. Watson, C. J., and Miller, W. R. (1995) *British Journal of Cancer* **71**, 840-844
7. Garcia, R., Bowman, T. L., Niu, G., Yu, H., Minton, S., Muro-Cacho, C. A., Cox, C. E., Falcone, R., Fairclough, R., Parsons, S., Laudano, A., Gazit, A., Levitzki, A., Kraker, A., and Jove, R. (2001) *Oncogene* **20**, 2499-2513
8. Widschwendter, A., Tonko-Geymayer, S., Welte, T., Daxenbichler, G., Marth, C., and Doppler, W. (2002) *Clinical Cancer Research* **8**, 3065-3074
9. Bratthauer, G. L., and Tavassoli, F. A. (2001) *Breast Cancer Research & Treatment* **69**, 295
10. Berclaz, G., Altermatt, H. J., Rohrbach, V., Siragusa, A., Dreher, E., and Smith, P. D. (2001) *International Journal of Oncology* **19**, 1155-1160

11. Dolled-Filhart, M., Camp, R. L., Kowalski, D. P., Smith, B. L., and Rimm, D. L. (2003) *Clin Cancer Res* **9**, 594-600
12. Dolled-Filhart, M., and Rimm, D. L. (2002) *Principles and Practices of Oncology* **16**, 1-11
13. Sorlie, T., Perou, C. M., Tibshirani, R., Aas, T., Geisler, S., Johnsen, H., Hastie, T., Eisen, M. B., van de Rijn, M., Jeffrey, S. S., Thorsen, T., Quist, H., Matese, J. C., Brown, P. O., Botstein, D., Eystein Lonning, P., and Borresen-Dale, A. L. (2001) *Proc Natl Acad Sci U S A* **98**, 10869-10874
14. Perou, C. M., Jeffrey, S. S., van de Rijn, M., Rees, C. A., Eisen, M. B., Ross, D. T., Pergamenschikov, A., Williams, C. F., Zhu, S. X., Lee, J. C., Lashkari, D., Shalon, D., Brown, P. O., and Botstein, D. (1999) *Proc Natl Acad Sci U S A* **96**, 9212-9217
15. Meric, F., Lee, W. P., Sahin, A., Zhang, H., Kung, H. J., and Hung, M. C. (2002) *Clin Cancer Res* **8**, 361-367
16. Mellick, A. S., Day, C. J., Weinstein, S. R., Griffiths, L. R., and Morrison, N. A. (2002) *International Journal of Cancer* **100**, 172-180
17. Lai, K. S., Jin, Y., Graham, D. K., Witthuhn, B. A., Ihle, J. N., and Liu, E. T. (1995) *J Biol Chem* **270**, 25028-25036
18. Zhou, Y., Wang, S., Gobl, A., and Oberg, K. (2001) *Oncology* **60**, 330-338
19. Chen, W. S., Kung, H. J., Yang, W. K., and Lin, W. (1999) *International Journal of Cancer* **83**, 579-584
20. Nemoto, T., Ohashi, K., Akashi, T., Johnson, J. D., and Hirokawa, K. (1997) *Pathobiology* **65**, 195-203
21. Watanabe, G., Kaganoi, J., Imamura, M., Shimada, Y., Itami, A., Uchida, S., Sato, F., and Kitagawa, M. (2001) *Cancer J* **7**, 132-139
22. Liu, P., Kimmoun, E., Legrand, A., Sauvanet, A., Degott, C., Lardeux, B., and Bernuau, D. (2002) *J Hepatol* **37**, 63-71
23. Feng, D. Y., Zheng, H., Tan, Y., and Cheng, R. X. (2001) *World J Gastroenterol* **7**, 33-36
24. Wei, D., Le, X., Zheng, L., Wang, L., Frey, J. A., Gao, A. C., Peng, Z., Huang, S., Xiong, H. Q., Abbruzzese, J. L., and Xie, K. (2003) *Oncogene* **22**, 319-329
25. Savarese, T. M., Campbell, C. L., McQuain, C., Mitchell, K., Guardiani, R., Quesenberry, P. J., and Nelson, B. E. (2002) *Cytokine* **17**, 324-334
26. Yasuda, Y., Fujita, Y., Masuda, S., Musha, T., Ueda, K., Tanaka, H., Fujita, H., Matsuo, T., Nagao, M., Sasaki, R., and Nakamura, Y. (2002) *Carcinogenesis* **23**, 1797-1805
27. Hough, C. D., Cho, K. R., Zonderman, A. B., Schwartz, D. R., and Morin, P. J. (2001) *Cancer Res* **61**, 3869-3876
28. Chen, H., Lee, J. M., Zong, Y., Borowitz, M., Ng, M. H., Ambinder, R. F., and Hayward, S. D. (2001) *J Virol* **75**, 2929-2937
29. Xie, L., Xu, L., He, Z., Zhou, W., Wang, L., Zhang, L., Lan, K., Ren, C., Liu, W., and Yao, K. (2000) *Journal of Cancer Research & Clinical Oncology* **126**, 400-406
30. Grandis, J. R., Drenning, S. D., Zeng, Q., Watkins, S. C., Melhem, M. F., Endo, S., Johnson, D. E., Huang, L., He, Y., and Kim, J. D. (2000) *Proceedings of the National Academy of Sciences of the United States of America* **97**, 4227-4232
31. Nagpal, J. K., Mishra, R., and Das, B. R. (2002) *Cancer* **94**, 2393-2400
32. Masuda, M., Suzui, M., Yasumatu, R., Nakashima, T., Kuratomi, Y., Azuma, K., Tomita, K., Komiyama, S., and Weinstein, I. B. (2002) *Cancer Research* **62**, 3351-3355
33. Agarwala, S. S., and Kirkwood, J. M. (2002) *Oncology (Huntingt)* **16**, 1177-1187; discussion 1190-1172, 1197

34. Gray, R. J., Pockaj, B. A., and Kirkwood, J. M. (2002) *Cancer Control* **9**, 16-21
35. Niu, G., Bowman, T., Huang, M., Shivers, S., Reintgen, D., Daud, A., Chang, A., Kraker, A., Jove, R., and Yu, H. (2002) *Oncogene* **21**, 7001-7010
36. Chawla-Sarkar, M., Leaman, D. W., Jacobs, B. S., Tuthill, R. J., Chatterjee-Kishore, M., Stark, G. R., and Borden, E. C. (2002) *Journal of Interferon & Cytokine Research* **22**, 603-613
37. Carson, W. E. (1998) *Clin Cancer Res* **4**, 2219-2228
38. Kirkwood, J. M., Farkas, D. L., Chakraborty, A., Dyer, K. F., Tweardy, D. J., Abernethy, J. L., Edington, H. D., Donnelly, S. S., and Becker, D. (1999) *Mol Med* **5**, 11-20
39. Clifford, J. L., Menter, D. G., Yang, X., Walch, E., Zou, C., Clayman, G. L., Schaefer, T. S., El-Naggar, A. K., Lotan, R., and Lippman, S. M. (2000) *Cancer Epidemiol Biomarkers Prev* **9**, 993-997
40. Mora, L. B., Buettner, R., Seigne, J., Diaz, J., Ahmad, N., Garcia, R., Bowman, T., Falcone, R., Fairclough, R., Cantor, A., Muro-Cacho, C., Livingston, S., Karras, J., Pow-Sang, J., and Jove, R. (2002) *Cancer Research* **62**, 6659-6666
41. Dhir, R., Ni, Z., Lou, W., DeMiguel, F., Grandis, J. R., and Gao, A. C. (2002) *Prostate* **51**, 241-246
42. Campbell, C. L., Jiang, Z., Savarese, D. M., and Savarese, T. M. (2001) *American Journal of Pathology* **158**, 25-32
43. Giri, D., Ozen, M., and Ittmann, M. (2001) *Am J Pathol* **159**, 2159-2165
44. Ni, Z., Lou, W., Lee, S. O., Dhir, R., DeMiguel, F., Grandis, J. R., and Gao, A. C. (2002) *Journal of Urology* **167**, 1859-1862
45. Chott, A., Sun, Z., Morganstern, D., Pan, J., Li, T., Susani, M., Mosberger, I., Upton, M. P., Bubley, G. J., and Balk, S. P. (1999) *Am J Pathol* **155**, 1271-1279
46. Horiguchi, A., Oya, M., Shimada, T., Uchida, A., Marumo, K., and Murai, M. (2002) *Journal of Urology* **168**, 762-765
47. Garcia, J. F., Camacho, F. I., Morente, M., Fraga, M., Montalban, C., Bellas, T. A., Castano, A., Diez, A., Flores, T., Martin, C., Martinez, M. A., Mazorra, F., Menarguez, J., Mestre, M. J., Mollejo, M., Saez, A. I., Sanchez, L., and Piris, M. A. (2003) *Blood* **101**, 681-689
48. Hinz, M., Lemke, P., Anagnostopoulos, I., Hacker, C., Krappmann, D., Mathas, S., Dorken, B., Zenke, M., Stein, H., and Scheidereit, C. (2002) *J Exp Med* **196**, 605-617
49. Zamo, A., Chiarle, R., Piva, R., Howes, J., Fan, Y., Chilosi, M., Levy, D. E., and Inghirami, G. (2002) *Oncogene* **21**, 1038-1047
50. Qin, J. Z., Kamarashev, J., Zhang, C. L., Dummer, R., Burg, G., and Dobbeling, U. (2001) *J Invest Dermatol* **117**, 583-589
51. Zhang, Q., Nowak, I., Vonderheid, E. C., Rook, A. H., Kadin, M. E., Nowell, P. C., Shaw, L. M., and Wasik, M. A. (1996) *Proc Natl Acad Sci U S A* **93**, 9148-9153
52. Wessendorf, S., Schwaenen, C., Kohlhammer, H., Kienle, D., Wrobel, G., Barth, T. F., Nessling, M., Moller, P., Dohner, H., Lichter, P., and Bentz, M. (2003) *Oncogene* **22**, 1425-1429
53. Zhu, Y., Hollmen, J., Raty, R., Aalto, Y., Nagy, B., Elonen, E., Kere, J., Mannila, H., Franssila, K., and Knuutila, S. (2002) *Br J Haematol* **119**, 905-915
54. Lai, R., Rassidakis, G. Z., Medeiros, L. J., Leventaki, V., Keating, M., and McDonnell, T. J. (2003) *J Pathol* **199**, 84-89
55. Skinnider, B. F., Elia, A. J., Gascoyne, R. D., Patterson, B., Trumper, L., Kapp, U., and Mak, T. W. (2002) *Blood* **99**, 618-626

56. Catlett-Falcone, R., Landowski, T. H., Oshiro, M. M., Turkson, J., Levitzki, A., Savino, R., Ciliberto, G., Moscinski, L., Fernandez-Luna, J. L., Nunez, G., Dalton, W. S., and Jove, R. (1999) *Immunity* **10**, 105-115
57. Benekli, M., Xia, Z., Donohue, K. A., Ford, L. A., Pixley, L. A., Baer, M. R., Baumann, H., and Wetzler, M. (2002) *Blood* **99**, 252-257
58. Biethahn, S., Alves, F., Wilde, S., Hiddemann, W., and Spiekermann, K. (1999) *Experimental Hematology* **27**, 885-894
59. Hayakawa, F., Towatari, M., Iida, H., Wakao, H., Kiyoi, H., Naoe, T., and Saito, H. (1998) *Br J Haematol* **101**, 521-528
60. Schuringa, J. J., Wierenga, A. T., Kruijer, W., and Vellenga, E. (2000) *Blood* **95**, 3765-3770
61. Gouilleux-Gruart, V., Gouilleux, F., Desaint, C., Claisse, J. F., Capiod, J. C., Delobel, J., Weber-Nordt, R., Dusanter-Fourt, I., Dreyfus, F., Groner, B., and Prin, L. (1996) *Blood* **87**, 1692-1697
62. Testa, U., Riccioni, R., Militi, S., Coccia, E., Stellacci, E., Samoggia, P., Latagliata, R., Mariani, G., Rossini, A., Battistini, A., Lo-Coco, F., and Peschle, C. (2002) *Blood* **100**, 2980-2988
63. Weber-Nordt, R. M., Egen, C., Wehinger, J., Ludwig, W., Gouilleux-Gruart, V., Mertelsmann, R., and Finke, J. (1996) *Blood* **88**, 809-816
64. Frank, D. A., Mahajan, S., and Ritz, J. (1997) *J Clin Invest* **100**, 3140-3148
65. Xia, Z., Sait, S. N., Baer, M. R., Barcos, M., Donohue, K. A., Lawrence, D., Ford, L. A., Block, A. M., Baumann, H., and Wetzler, M. (2001) *Leukemia Research* **25**, 473-482
66. Chai, S. K., Nichols, G. L., and Rothman, P. (1997) *J Immunol* **159**, 4720-4728
67. Landolfo, S., Guarini, A., Riera, L., Gariglio, M., Gribaudo, G., Cignetti, A., Cordone, I., Montefusco, E., Mandelli, F., and Foa, R. (2000) *Hematol J* **1**, 7-14
68. Bruchova, H., Borovanova, T., Klamova, H., and Brdicka, R. (2002) *Leukemia & Lymphoma* **43**, 1289-1295
69. Vallat, L., Magdelenat, H., Merle-Beral, H., Masdehors, P., Potocki De Montalk, G., Davi, F., Kruhoffer, M., Sabatier, L., Orntoft, T. F., and Delic, J. (2003) *Blood*

Automated subcellular localization and quantification of protein expression in tissue microarrays

ROBERT L. CAMP, GINA G. CHUNG & DAVID L. RIMM
Department of Pathology, Yale University School of Medicine, New Haven, Connecticut, USA
Correspondence should be addressed to D.L.R.; email: david.rimm@yale.edu

Published online 21 October 2002; doi:10.1038/nm791

The recent development of tissue microarrays—composed of hundreds of tissue sections from different tumors arrayed on a single glass slide—facilitates rapid evaluation of large-scale outcome studies. Realization of this potential depends on the ability to rapidly and precisely quantify the protein expression within each tissue spot. We have developed a set of algorithms that allow the rapid, automated, continuous and quantitative analysis of tissue microarrays, including the separation of tumor from stromal elements and the sub-cellular localization of signals. Validation studies using estrogen receptor in breast carcinoma show that automated analysis matches or exceeds the results of conventional pathologist-based scoring. Automated analysis and sub-cellular localization of beta-catenin in colon cancer identifies two novel, prognostically significant tumor subsets, not detected by traditional pathologist-based scoring. Development of automated analysis technology empowers tissue microarrays for use in discovery-type experiments (more typical of cDNA microarrays), with the added advantage of inclusion of long-term demographic and patient outcome information.

Despite the promise of automated analysis of histological sections, it has failed to replace traditional, pathologist-based evaluation, even in the simplest of conditions such as the analysis of immunohistochemical stains. Whereas the automated analysis of isolated cells in fluids or smears (for example, fluorescent cell sorting and laser scan cytometry) is now routine[1], the analysis of tissue sections is hampered by the fact that tumor tissue is a complex mixture of overlapping malignant tumor cells, benign host-derived cells and extracellular material. Several methods (including confocal and convolution/deconvolution microscopy) can determine the subcellular localization of target antigens, but only through computationally intensive techniques, requiring the acquisition of multiple high-power, serial images[2]. Methods designed for tissue microarrays perform only limited subcellular localization using morphometry and usually require significant manual interface (for example, drawing polygons around tumor cells)[3,4]. In general, pathologist-based analysis remains the current standard for the immunohistochemical studies.

Tissue microarrays provide a high-throughput method of analyzing the prognostic benefit of a myriad of potential targets on large cohorts of patient samples[5–7], but are limited by the pathologist's ability to reproducibly score on a continuous scale, discriminate between subtle low-level staining differences, and accurately score expression within subcellular compartments. We have developed a set of algorithms that we call AQUA (Automated Quantitative Analysis) that allow the rapid, automated analysis of large-scale cohorts on tissue microarrays. The first algorithm, called PLACE (pixel-based locale assignment for compartmentalization of expression) utilizes fluorescent tags to separate tumors from stroma and to define subcellular compartments. The distribution of a target antigen is then quantitatively assessed according to its co-localization with these tags. As subcellular compartments (for example, membrane, cytoplasm, nuclei and so forth) of different tissues and tumors vary widely in size and shape, traditional methods of defining compartments based on morphometric criteria (that is, feature extraction) perform poorly on a large-scale basis. Rather than counting target-containing features, PLACE delineates target expression as the sum of its intensity divided by the total size of the assayed compartment.

As the thickness of tissue sections makes it difficult to discriminate between overlapping subcellular compartments, we have also developed a novel, rapid exponential subtraction algorithm (RESA), which subtracts an out-of-focus image, collected slightly below the bottom of the tissue, from an in-focus image, based on pixel intensity, signal-to-noise ratio, and the expected compartment size. This algorithm dramatically improves the assignment of pixels to a particular subcellular compartment (Fig. 1). For a more complete discussion of the image manipulations performed in this protocol, see Supplementary Methods or http://www.yalepath.org/dept/research/YC-CTMA/tisarray.htm.

Validation of AQUA algorithms

Our initial validation of this technology compared its accuracy, intra-observer variability, and predictive power to traditional pathologist-based analysis. We stained a tissue microarray derived from 340 node-positive breast-carcinoma patients for the presence of estrogen receptor (ER)—the oldest and most common prognostic marker for breast cancer[8]. First we analyzed the ability of automated analysis to match results from a pathologist-based evaluation and found a high degree of correlation ($R = 0.884$, Fig 2*a*). Next, we compared the variability of a pathologist-based and automated analysis of two separate histospots derived from the same tumor (Fig. 2*b* and *c*). This comparison shows that automated analysis has slightly better reproducibility ($R = 0.824$ versus $R = 0.732$).

Although automated analysis compares favorably with pathologist-based interpretation of microarrays, the true criterion standard is outcome prediction. Estrogen receptor expression is known to significantly improve outcome, because it is associated with less aggressive tumors that are more responsive to anti-estrogenics (for example, Tamoxifen). We compared the survival of patients with tumors with high (top 25%) versus low (bottom 25%) ER expression as assessed by both automated and pathologist-based scoring (Fig. 2*d*). Results show that both methods provide similar prognostic information ($RR = 2.44$ versus 2.06, automated versus pathologist); although the auto-

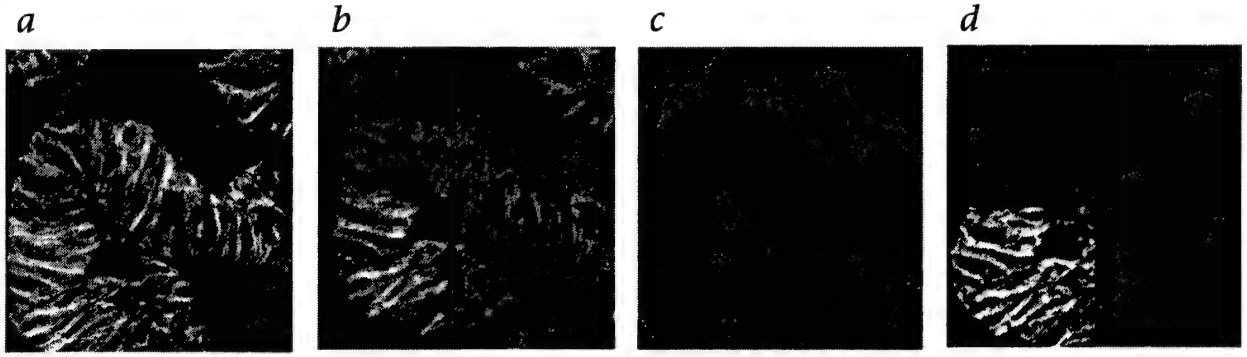

Fig. 1 RESA allows the accurate assignment of subcellular compartments and localization of a target antigen. ***a***, A pseudo three-color image of a colon carcinoma shows a significant degree of overlap between subcellular compartments: Blue, nuclei (DAPI); green, tumor mask (cytokeratin); red, tumor cell membranes (alpha-catenin). ***b***, The signal intensity of a target antigen, β-catenin (inset), is redistributed according to the relative signal intensity of the compartments identified in *a*: Blue, nuclear-localized; red, membrane-localized; green, cytoplasmic. Note that the β-catenin expression in this tumor is predominantly membrane-associated, yet there is significant incorrectly assigned signal in the nucleus: magenta and blue pixels. ***c***, The compartment-specific signals in *a* are reassigned using the RESA algorithm, reducing the amount of overlapping signal by exponentially subtracting pixel intensity from an out-of-focus image. ***d***, The signal intensity from an exponentially subtracted image of the target antigen, β-catenin (inset) is then redistributed according to the compartments defined in *c*. This results in more accurate assignment of the target antigen to the membrane compartment (red pixels) with little expression in the nuclear compartment (blue pixels).

mated analysis shows slightly higher significance ($P = 0.0003$ versus $P = 0.0020$). Univariate analysis of the automated analysis shows a relative risk of 2.438 ($P = 0.0005$, 95% CI 1.480–4.016). When analyzed in a multivariate analysis against histological and nuclear grades, age and stage, automated ER analysis retains independent prognostic significance (RR = 2.566, 95% CI 1.428–4.611, $P = 0.0016$). The pathologist-based analysis shows similar results, validating the cohort (see Supplementary Methods).

To determine the reproducibility of our automated analysis of ER, we used the 'split-sample technique,' by dividing the cohort into halves and using one half as a 'training' set and the other as a 'test' set[9]. The training set was used to determine standard cutoffs for the top and bottom 25% of cases. These cutoffs were then used to divide the test set into top, middle and bottom groups. We analyzed 300 randomly selected training and test sets; on average 97% of the test cases were correctly classified.

One clear advantage to automated analysis is that it can perform a true continuous assessment of a target. In contrast, the human eye, even that of a trained pathologist, has a difficult time accurately distinguishing subtle differences in staining intensity using a continuous scale. Consequently, scoring systems for pathologists tend to be nominal (for example, 0, 1+, 2+, 3+). Algorithms such as the 'H-score' are meant to translate such nominal observations into semi-quantitative results. However, the inability to detect subtle differences in staining intensity, particularly at the low and high ends of the scale, as well as the tendency to round scores limits the effectiveness of the H-score. The discontinuity of pathologist-based scoring, despite the use of an H-score algorithm, is exemplified in the

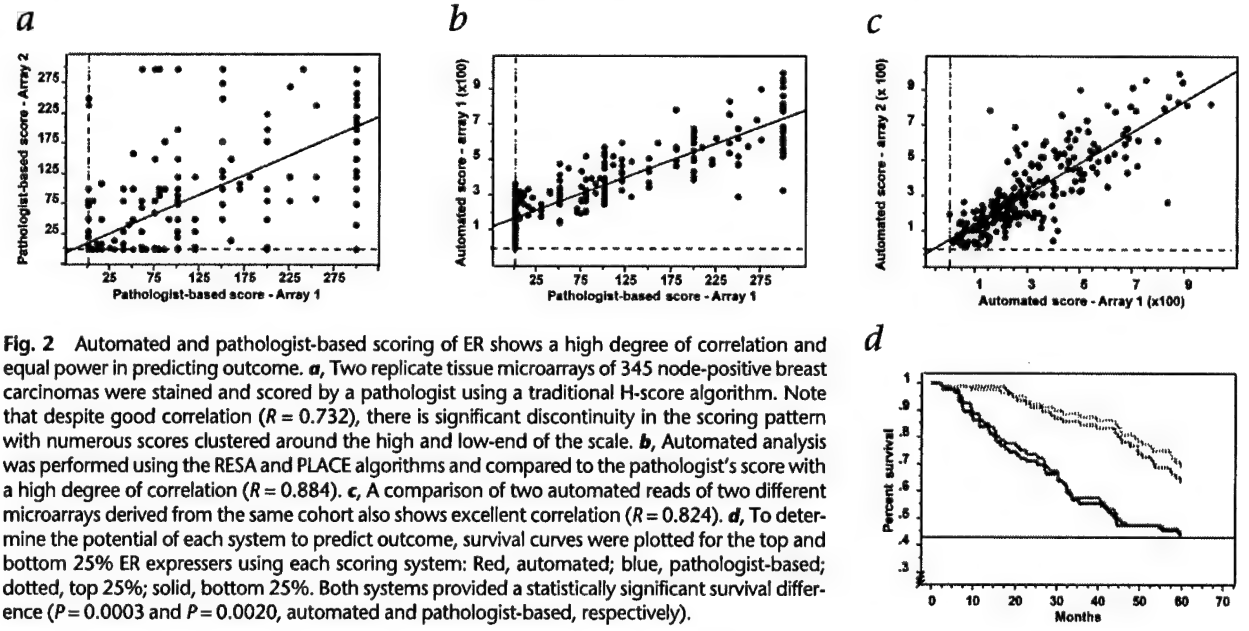

Fig. 2 Automated and pathologist-based scoring of ER shows a high degree of correlation and equal power in predicting outcome. ***a***, Two replicate tissue microarrays of 345 node-positive breast carcinomas were stained and scored by a pathologist using a traditional H-score algorithm. Note that despite good correlation ($R = 0.732$), there is significant discontinuity in the scoring pattern with numerous scores clustered around the high and low-end of the scale. ***b***, Automated analysis was performed using the RESA and PLACE algorithms and compared to the pathologist's score with a high degree of correlation ($R = 0.884$). ***c***, A comparison of two automated reads of two different microarrays derived from the same cohort also shows excellent correlation ($R = 0.824$). ***d***, To determine the potential of each system to predict outcome, survival curves were plotted for the top and bottom 25% ER expressers using each scoring system: Red, automated; blue, pathologist-based; dotted, top 25%; solid, bottom 25%. Both systems provided a statistically significant survival difference ($P = 0.0003$ and $P = 0.0020$, automated and pathologist-based, respectively).

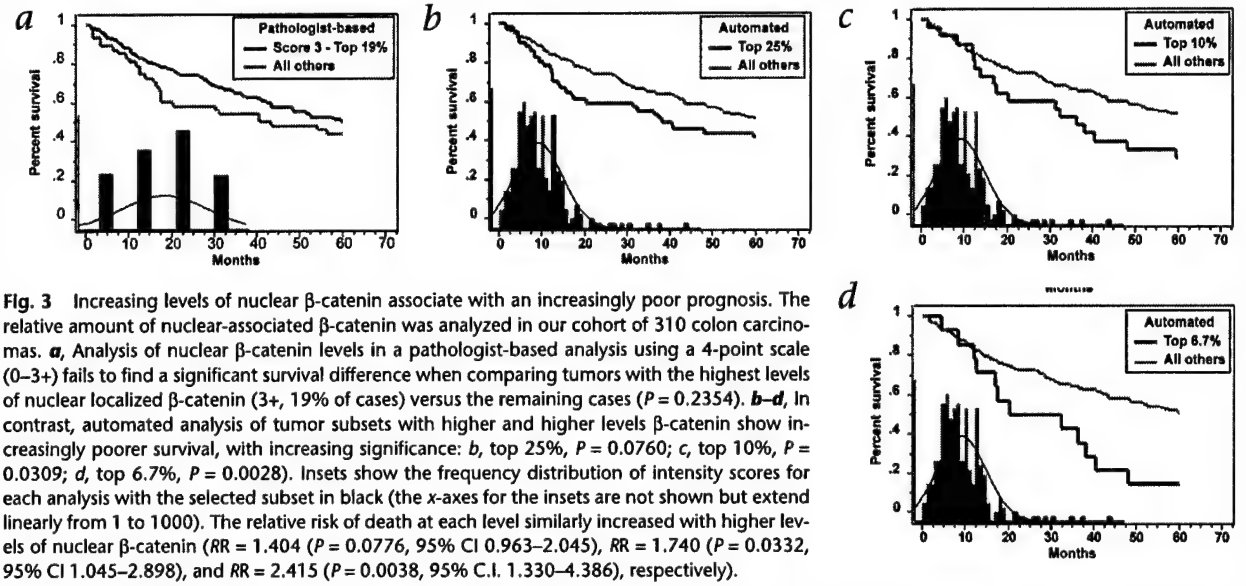

Fig. 3 Increasing levels of nuclear β-catenin associate with an increasingly poor prognosis. The relative amount of nuclear-associated β-catenin was analyzed in our cohort of 310 colon carcinomas. ***a***, Analysis of nuclear β-catenin levels in a pathologist-based analysis using a 4-point scale (0–3+) fails to find a significant survival difference when comparing tumors with the highest levels of nuclear localized β-catenin (3+, 19% of cases) versus the remaining cases ($P = 0.2354$). ***b–d***, In contrast, automated analysis of tumor subsets with higher and higher levels β-catenin show increasingly poorer survival, with increasing significance: *b*, top 25%, $P = 0.0760$; *c*, top 10%, $P = 0.0309$; *d*, top 6.7%, $P = 0.0028$). Insets show the frequency distribution of intensity scores for each analysis with the selected subset in black (the *x*-axes for the insets are not shown but extend linearly from 1 to 1000). The relative risk of death at each level similarly increased with higher levels of nuclear β-catenin (*RR* = 1.404 ($P = 0.0776$, 95% CI 0.963–2.045), *RR* = 1.740 ($P = 0.0332$, 95% CI 1.045–2.898), and *RR* = 2.415 ($P = 0.0038$, 95% C.I. 1.330–4.386), respectively).

ER staining results in Fig. 2. Note the preponderance of scores at 0, 100, 200 and 300. Furthermore, on average, over half of the cases were assigned to one extreme or the other (39% at 0 and 12% at 300). Thus 51% of the cases could not be effectively ranked. In contrast, the range of scores from the automated analysis is continuous from 0 to 1000. We hypothesize that the two key advantages of automated assessment, continuity of scoring and accurate subcellular localization, will allow tumor classification beyond that attainable by current methods.

Compartmental analysis of beta-catenin expression

To demonstrate this potential, we analyzed β-catenin expression in colon cancer. β-catenin is an ideal candidate in that it exhibits complex subcellular localization and manifests oncogenic properties upon localization to the nucleus[10]. Numerous studies have shown that β-catenin plays a dual role in both cell–cell adhesion and cell proliferation, depending on its location[11]. Membrane-associated β-catenin stabilizes cadherins-mediated adhesion by facilitating the cytoskeletal attachment of adhesion complexes. In contrast, nuclear-associated β-catenin activates several genes important in cell proliferation and invasion[12]. In development, translocation of β-catenin to the nucleus results from *wnt*-mediated cell signaling[13]. However, spurious activation of this pathway is often seen in tumors through mutation of β-catenin or other proteins involved in its activation and/or degradation[14]. Studies on the prognostic value of β-catenin have been mixed[15–17].

The complex biology and uncertain prognostic value of β-catenin made it a suitable candidate for assessing the value of quantitative subcellular localization. We studied a cohort of 310 colon cancers, using both pathologist-based and automated systems for scoring overall, nuclear and membrane-associated levels of β-catenin expression. Manual analysis used a traditional 4-point nominal scale (0 through 3+), whereas automated analysis used a continuous 1,000-point scale. In a previous study using a similar cohort, we were unable to find prognostic value in assessing nuclear β-catenin levels[18]. These data were confirmed in our present study when comparing tu-

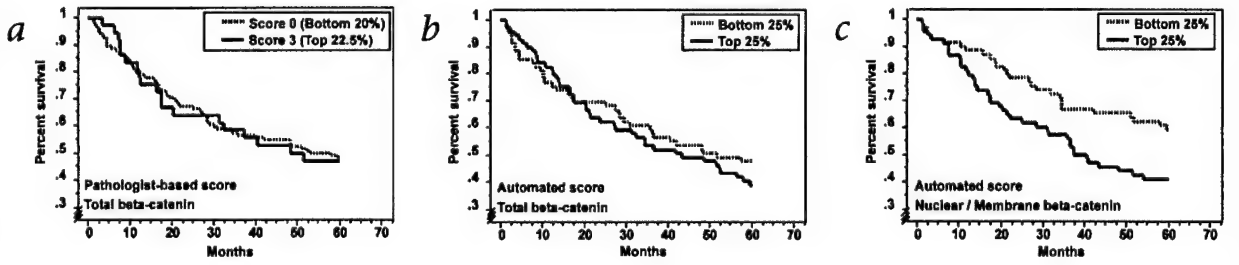

Fig. 4 Unlike analyses of overall β-catenin expression, automated, subcellular localization of β-catenin can predict outcome in colon carcinoma. ***a***, Overall β-catenin levels in a cohort of 310 colon cancers were evaluated by a pathologist using a 4-point scale (0–3+). Survival analysis of tumors with the lowest (0) versus highest (3+) overall β-catenin expression was not significant ($P = 0.9425$). ***b***, Similarly, automated analysis of overall β-catenin levels, comparing cases in the top and bottom 25%, failed to detect a survival difference ($P = 0.4551$). ***c***, In contrast, the ratio of nuclear to membrane β-catenin, as assessed by automated analysis, demonstrates that tumors with higher relative nuclear expression do worse than those with higher relative membrane expression ($P = 0.0264$, top versus bottom 25% of cases, *RR* = 1.718, 95% CI = 1.059–2.787). Note that the nuclear/membrane ratio identifies a large subset (25%) of tumors with poor prognosis, the majority of which are not identified by analyzing individual subcellular compartments. Indeed, comparison of tumors with high nuclear/membrane ratios (top 25%) versus those with high nuclear β-catenin (top 25%) shows that there is only 47% overlap.

mors expressing the highest levels of nuclear β-catenin (3+, representing 19% of the cases) versus the rest (Fig 3*a*) (P = 0.2354). We hypothesized that with the benefit of automated, continuous assessment, these 3+ cases could be subdivided into cases expressing very high versus high levels. We began by analyzing the top 25% of tumors expressing nuclear β-catenin, as assessed by automated analysis. This group shows a trend toward poorer survival (Fig 3*b*) (P = 0.0760). When we subset the tumors to assess the top 10% expressers, there is a statistically significant survival difference (Fig. 3*c*) (P = 0.0332, relative risk = 1.740). Further fractionation of the data reveals that the top 6.7% (15th percentile) exhibit even poorer survival with a higher statistical significance (Fig. 3*d*) (P = 0.0038, relative risk = 2.415). This analysis demonstrates the power of continuous automated assessment to define subsets of tumors not seen using standard pathologist-based assessment. Unlike β-catenin, subdividing ER into smaller and smaller subsets does not significantly alter its prognostic ability, suggesting that ER may be a truly continuous marker where no subpopulations exist.

Tumor classification using the AQUA algorithms

We then attempted a tumor classification based on comparative subcellular localization. As the translocation of β-catenin from the membrane to the nucleus is thought to correlate with transcriptional activation, we analyzed the ratio of nuclear to membrane-localized β-catenin. By its nature, this type of analysis is essentially impossible without continuous scoring. A crude measurement of overall β-catenin levels using either a pathologist-based or an automated system fails to demonstrate a significant difference in survival between the highest and lowest expressing tumors (Fig. 4, *a* and *b*, P = 0.9425 and P = 0.4551, respectively). In contrast, when we ratio the level of nuclear/membrane β-catenin, we find that tumors with a high ratio have a worse outcome than tumors with a low ratio (RR = 1.718, P = 0.0284). Note that this method defines a relatively large subset (25%) of tumors with poor prognosis, the majority of which are not identified by analyzing individual subcellular compartments. Indeed, a comparison of the tumors with the highest nuclear/membrane ratio (top 25%) versus the highest overall nuclear levels of β-catenin (top 25%) shows that there is only 47% overlap between the two subsets. Multivariate analysis of nuclear/membrane β-catenin ratios shows independent prognostic significance when analyzed with depth of invasion, nodal status, tumor grade and patient age (RR = 1.865, 95% CI = 1.068–3.259, P = 0.0285). In contrast, multivariate analysis of total nuclear β-catenin levels fails to show independent prognostic significance because it is highly correlated with nodal metastases (see Supplementary Methods online).

The methods presented here are highly adaptable to a number of tumor types and target markers. In most cases, compartment-specific tags are identical regardless of tumor type (DAPI for nuclei, cadherins/catenin complexes for membranes). Because the methods do not use heuristic models that require recognition of compartments according to size, shape or texture, they are fully adaptable to tumors with overlapping or pleomorphic cells and/or nuclei. Furthermore, the algorithms can be easily expanded to cover novel compartments or even 'virtual' compartments (for example, mitochondria, lysosomes, cortical actin ring) or tumor types (for example, mesothelioma), as long as tags can be identified for the prospective compartments/cell types. In addition to ER and β-catenin, we have used these techniques to successfully analyze dozens of markers, including growth factor receptors, intracellular signaling molecules, and proliferation markers, using both conventional and phospho-specific antibodies (see Supplementary Methods online). Analysis of these targets requires only a standard antibody titration.

We have found that most antigens benefit from subcellular localization. Localization can be simple, such as determining the amount of the proliferation marker KI-67 in tumor nuclei, or more complex as in the case of β-catenin. Localization of intracellular signaling molecules (for example, STATs) may be vital in assessing their potential as prognostic markers. In addition, recent studies have shown that membrane-bound growth factor receptors (for example, epidermal growth factors, EGFR and ERB-B4, and fibroblast growth factor) can translocate to the nucleus and may act as transcriptional regulators[19]. Subcellular localization of such markers may be critical to their use as prognostic markers in cancer.

Depending upon the array size, and the complexity of the compartmentalization, analyses using our current device take from 1–3 hours for image acquisition, and 1–2 hours for analysis. In our laboratory, the average pathologist-based analysis rate is 50–100 spots per hour and usually is performed in several sessions. To increase precision, two or more pathologists read the same array independently and then together to resolve discrepancies. Aside from being more accurate and more robust, automated analysis can be performed continuously and results tabulated immediately. We estimate that a fully integrated tissue microarray reader could be 30 to 50 times faster than pathologist-based scoring.

Methods

Tissue microarray design and processing. Paraffin-embedded formalin-fixed specimens from 345 cases of node-positive breast carcinoma (1962–1977) and 310 cases of colon carcinoma (1971–1982) were obtained, as available, from the archives of the Yale University Department of Pathology. Microarray slides were prepared, processed and stained as described in the Supplementary Methods online. For manual analysis, slides were visualized with diaminobenzidine (DAB). For automated analysis, slides were visualized with Cy-5 tyramide.

Image and data analysis. Monochromatic images of tissue microarray histospots were obtained using fluorescently labeled compartment specific tags (anti-cytokeratin, DAPI, α-catenin) as well as target signals (ER and β-catenin). Regions of tumor were identified using a mask derived from a ubiquitously expressed epithelial-specific antigen (either cytokeratin or α-catenin). Images were analyzed using RESA and PLACE algorithms as detailed in the Supplementary Methods online. Results were expressed as the intensity of the target signal in each compartment divided by the compartment. For ER, only nuclear-localized signal was used; for β-catenin total signal, the ratios of nuclear-to-membrane signal and nuclear-to-total signal were analyzed. Overall survival analysis was assessed using Kaplan–Meier analysis and the Mantel–Cox log-rank score for assessing statistical significance. Relative risk was assessed using the univariate and multivariate Cox-proportional hazards model.

Our data show that quantitative, continuous-scale, compartmentalized automated analysis of tissue microarrays can provide a rapid assessment of prognosis-based subsets in a variety of tumor markers that cannot be attained using pathologist-based techniques. Automated analysis is better able to discern subtle differences in staining intensity, particularly at the upper and lower extremes, which can distinguish novel prognostic associations. Furthermore, analysis of the subcellular distribution of certain signals, using the PLACE and RESA algorithms may elucidate previously unrecognized associations with patient survival. The automated nature of this technology can allow high-throughput screening of tissue microarrays, facilitating their use in large-scale, high-throughput applications such as target discovery and prognostic marker validation. If, someday, diagnostic criteria are based on molecular expression patterns, the digital nature of this analysis could allow a device of this type to make specific molecular diagnoses.

Note: Supplementary information available on the Nature Medicine *website.*

Acknowledgments

We thank T. D'Aquila, M. Helie, L. Charette, D. Fischer, E. Rimm and P. Lizardi for their help in this effort; and J. Costa, V. Marchesi, A. Reynolds, R. Levenson and E. Fearon for review of the manuscript. This work was supported by grants from the Patrick and Catherine Weldon Donaghue Foundation for Medical Research and grants from the NIH including: K0-8 ES11571, NIEHS (to R.L.C.), RO-1 GM57604 NCI (to D.L.R.) and US Army DAMD grant 01-000436.

Competing interests statement

The authors declare competing financial interests: see the website (http://nature.com/naturemedicine

1. Tarnok, A. & Gerstner, A.O. Clinical applications of laser scanning cytometry. *Cytometry* **50**, 133–143 (2002).
2. Robinson, J.P. Principles of confocal microscopy. *Methods Cell Biol.* **63**, 89–106 (2001).
3. Rao, J., Seligson, D. & Hemstreet, G.P. Protein expression analysis using quantitative fluorescence image analysis on tissue microarray slides. *Biotechniques* **32**, 924–932 (2002).
4. Bacus, S. *et al.* Potential use of image analysis for the evaluation of cellular predicting factors for therapeutic response in breast cancers. *Anal. Quant. Cytol. Histol.* **19**, 316–328 (1997).
5. Kallioniemi, O.P., Wagner, U., Kononen, J. & Sauter, G. Tissue microarray technology for high-throughput molecular profiling of cancer. *Hum. Mol. Genet.* **10**, 657–662 (2001).
6. Kononen, J. *et al.* Tissue microarrays for high-throughput molecular profiling of tumor specimens. *Nature Med.* **4**, 844–847 (1998).
7. Rimm, D.L. *et al.* Tissue microarray: a new technology for amplification of tissue resources. *Cancer J* **7**, 24–31 (2001).
8. Osborne, C.K. *et al.* Estrogen receptor, a marker for human breast cancer differentiation and patient prognosis. *Adv. Exp. Med. Biol.* **138**, 377–385 (1981).
9. Wasson, J.H., Sox, H.C., Neff, R.K. & Goldman, L. Clinical prediction rules. Applications and methodological standards. *N. Engl. J. Med.* **313**, 793–799 (1985).
10. Kobayashi, M. *et al.* Nuclear translocation of β-catenin in colorectal cancer. *Br. J. Cancer* **82**, 1689–1693 (2000).
11. Provost, E. & Rimm, D.L. Controversies at the cytoplasmic face of the cadherin-based adhesion complex. *Curr. Opin. Cell Biol.* **11**, 567–572 (1999).
12. Morin, P.J. β-catenin signaling and cancer. *Bioessays* **21**, 1021–1030 (1999).
13. Peifer, M. & Polakis, P. Wnt signaling in oncogenesis and embryogenesis—a look outside the nucleus. *Science* **287**, 1606–1609 (2000).
14. Wong, C.M., Fan, S.T. & Ng, I.O. β-catenin mutation and overexpression in hepatocellular carcinoma: clinicopathologic and prognostic significance. *Cancer* **92**, 136–145 (2001).
15. Gunther, K. *et al.* Predictive value of nuclear β-catenin expression for the occurrence of distant metastases in rectal cancer. *Dis. Colon Rectum* **41**, 1256–1261 (1998).
16. Maruyama, K. *et al.* Cytoplasmic β-catenin accumulation as a predictor of hematogenous metastasis in human colorectal cancer. *Oncology* **59**, 302–309 (2000).
17. Hugh, T.J. *et al.* Beta-catenin expression in primary and metastatic colorectal carcinoma. *Int. J. Cancer* **82**, 504–511 (1999).
18. Chung, G.G. *et al.* Tissue microarray analysis of β-catenin in colorectal cancer shows nuclear phospho-β-catenin is associated with a better prognosis. *Clin. Cancer Res.* **7**, 4013–4020 (2001).
19. Lin, S.Y. *et al.* Nuclear localization of EGF receptor and its potential new role as a transcription factor. *Nature Cell Biol.* **3**, 802–808 (2001).

[CANCER RESEARCH 63, 1445–1448, April 1, 2003]

Advances in Brief

Quantitative Analysis of Breast Cancer Tissue Microarrays Shows That Both High and Normal Levels of HER2 Expression Are Associated with Poor Outcome[1]

Robert L. Camp,[2] Marisa Dolled-Filhart, Bonnie L. King, and David L. Rimm

Departments of Pathology [R. L. C., D. L. R.], Genetics [M. D-F.], and Therapeutic Radiology [B. L. K.], Yale University, School of Medicine, New Haven, Connecticut 06520

Abstract

Using a tissue microarray cohort of 300 breast cancers and 84 samples of normal breast epithelium, we analyzed HER2/*neu* expression and compared traditional clinical (manual) scoring with a recently developed system for the quantitative measurement of immunohistochemical stains (AQUA). As expected, both methods identified a population (10–15%) of high-HER2-expressing tumors with poor 30-year disease-related survival. Using AQUA analysis, we found that normal epithelium expresses a low but detectable level of HER2 and that 17.5% of tumors exhibit similar low-level HER2 expression. This low group was not definable by manual scoring. Surprisingly, HER2-normal tumors were as aggressive as HER2-overexpressing tumors. Our studies suggest that *in situ* quantitative measurement of HER2 stratifies breast tumors into three expression levels: normal, intermediate, and high, where both normal and high levels are associated with a worse outcome.

Introduction

HER2 (*neu* or erb-B2), a member of the epidermal growth factor family, is genetically amplified and overexpressed in aggressive breast cancers. High levels of HER2 are associated with poor prognosis, particularly in node-positive breast carcinoma patients. Recently, a targeted therapeutic against HER2 has been developed. Trastuzumab (Herceptin) is a humanized monoclonal antibody directed against the extracellular domain of HER2. Treatment of patients with metastatic breast carcinoma with Herceptin has shown therapeutic benefit, especially when combined with conventional chemotherapeutic agents. The association between HER2 expression and Herceptin response has stimulated renewed interest in accurately assessing HER2 amplification and overexpression. Toward this goal, we have developed a system for compartmentalized, automated quantitative analysis of histological sections (AQUA; Ref. 1). As with an ELISA, AQUA provides highly reproducible analysis of target signal expression with use of a continuous, rather than nominal, scale. Unlike an ELISA, spatial information, including tissue and subcellular localization, is preserved. Using a tissue microarray composed of archival breast cancer specimens and normal epithelia, we found a bimodal distribution of HER2, where tumors expressing both high and normal HER2 levels exhibited poor 30-year disease-specific survival.

Materials and Methods

Tissue Microarray Design. Paraffin-embedded, formalin-fixed specimens from 300 cases of node-positive invasive breast carcinoma were identified from the archives of the Yale University Department of Pathology as available from 1962 to 1977, with a mean follow-up time of 9.6 years. No patients received Herceptin during the study period. Complete treatment information was unavailable for the entire cohort; however, most patients were treated with local radiation and ~15% were treated with chemotherapy consisting primarily of Adriamycin, cytoxan, and 5-fluorouracil. Approximately 27% subsequently received tamoxifen (post-1978). Seven patients had biopsy-proven stage IV disease at the time of diagnosis.

In constructing the microarrays, we identified areas of invasive carcinoma, away from *in situ* lesions and normal epithelium, and took two 0.6-mm cores. We cut 5-μm-thick sections of the microarrays and processed them as described previously (2, 3). We previously demonstrated with HER2 that two cores replicated the results of an entire slide in >95% of cases (4). An additional microarray consisting of 84 samples of normal epithelium was also constructed from samples of normal ducts and lobules taken from breast cancer patients. Samples were taken away from areas of tumor and assessed histologically to ensure that they were unaffected by atypical hyperplasia or carcinoma *in situ*.

Immunohistochemistry. Tissue microarray slides were stained as described (1). In brief, for both manual and automated analysis, slides were incubated for 1 h at room temperature with polyclonal anti-HER2 (1:200; DAKO Corp., Carpinteria, CA) diluted in Tris-buffered saline containing BSA. Previous analysis of titrations of the HER2 antibody demonstrated that higher dilutions of anti-HER2 antibody (1:1000~1:8000) more accurately define the HER2-high from the HER2-intermediate populations, whereas lower dilutions (1:50~1:500) distinguish the HER2-normal from HER2-intermediate populations.[3] In this study we used a concentration (1:200) that sufficiently distinguished all three populations. Goat antirabbit antibody conjugated to a horseradish peroxidase-decorated dextran polymer backbone (Envision; DAKO Corp.) was used as a secondary reagent. For manual analysis, slides were visualized with diaminobenzidine (DAKO Corp.), followed by ammonium hydroxide-acidified hematoxylin. For automated analysis, tumor cells were identified by use of a fluorescently tagged anticytokeratin antibody cocktail (AE1/AE3; DAKO Corp.). We added 4′,6-diamidino-2-phenylindole to visualize nuclei, and HER2 was visualized with a fluorescent chromogen (Cy-5-tyramide; NEN Life Science Products, Boston, MA). Cy-5 (red) was used because its emission peak is well outside the green-orange spectrum of tissue autofluorescence.

Automated Image Acquisition and Analysis. Automated image acquisition and analysis using AQUA has been described previously (1). In brief, monochromatic, high-resolution (1024 × 1024 pixel; 0.5-μm) images were obtained of each histospot. We distinguished areas of tumor from stromal elements by creating a mask from the cytokeratin signal. Coalescence of cytokeratin at the cell surface helped localize the cell membranes, and 4′,6-diamidino-2-phenylindole was used to identify nuclei. The HER2 signal from the membrane area of tumor cells was scored on a scale of 0–255 and expressed as signal intensity divided by the membrane area.

FISH. FISH[4] analysis was performed with the PathVysion HER2 DNA Probe Kit (Vysis, Downers Grove, IL), using two directly labeled fluorescent DNA probes complementary to the HER2/*neu* gene locus (LSI HER2/*neu* SpectrumRed) and to chromosome 17 pericentromeric α satellite DNA (CEP17 SpectrumGreen), according to standard protocols. HER2/*neu* gene amplification was quantified by comparing the ratio of LSI HER2/*neu* to CEP17 probe signals in accordance with the PathVysion HER2 DNA Probe Kit criteria. We examined 60 nonoverlapping tumor cell nuclei in each histo-

Received 11/6/02; accepted 2/14/03.

The costs of publication of this article were defrayed in part by the payment of page charges. This article must therefore be hereby marked *advertisement* in accordance with 18 U.S.C. Section 1734 solely to indicate this fact.

[1] This work was supported by grants from the Patrick and Catherine Weldon Donaghue Foundation for Medical Research, by grants from the NIH [K0-8 ES11571, NIEHS (to R. L. C.), and RO-1 GM57604 NCI (to D. L. R.)], the Greenwich Breast Cancer Alliance, and by United States Army DAMD Grant 01-000436.

[2] To whom requests for reprints should be addressed, at Department of Pathology, Yale University, School of Medicine, New Haven, CT 06520-8023.

[3] R. L. Camp, M. Dolled-Filhart, D. L. Rimm, unpublished observations.

[4] The abbreviation used is: FISH, fluorescence *in situ* hybridization.

spot to determine the average number of HER2/*neu* and chromosome 17 copies/cell for each tissue specimen. The ratio of these averages was used to determine the presence of HER2/*neu* gene amplification. Specimens with a HER2/*neu*:chromosome 17 ratio >2 were scored as positive for HER2/*neu* gene amplification.

Data Analysis. Manual scoring of HER2 expression was assessed by a pathologist (R. L. C.) using a nominal four-point scale (0 to 3+). Histospots containing <10% tumor, as assessed either subjectively (manual) or by mask area (automated), were excluded from further analysis. Previous studies have demonstrated that the staining from a single histospot provides a sufficiently representative sample for analysis (4, 5). Correlations with other prognostic markers were determined by χ^2 analysis. Overall survival analysis was assessed by Kaplan-Meier analysis with the Mantel-Cox log-rank score for determining statistical significance. Relative risk was assessed by the univariate and multivariate Cox proportional hazards model. Analyses were performed with Statview 5.0.1 (SAS Institute, Cary, NC). Patients were deemed "uncensored" if they died of breast cancer within 30 years of their initial date of diagnosis.

Results and Discussion

Validation of Microarray Cohort. To validate our tissue microarray cohort of 300 node-positive breast cancers, we assessed several traditional histopathological markers of malignancy. Using univariate analysis of long-term disease-related survival, we found that large tumor size, high nuclear grade, low estrogen receptor expression, and high number of involved lymph nodes were all significant predictors of poor outcome (Table 1). We next assessed the prognostic power of HER2 immunohistochemistry, using standard brown staining, visual examination by a pathologist, and scoring on a four-point scale (0 to 3+). Manual analysis showed a typical pattern of HER2 expression with 15% of tumors overexpressing the antigen (2+ and 3+; Fig. 1*B*). As expected, high-level (3+) tumors showed a significantly worse outcome with a relative risk of 2.25 ($P = 0.0007$; Table 1). Analysis of *HER2* gene amplification by FISH was not predictive in our study, but this was most likely attributable to the relatively small number of cases that, for technical reasons, were scorable (125 of 300; Table 1). However, both automated and manual analyses of HER2 protein levels were highly correlated with *HER2* gene amplification ($P < 0.0001$). The percentage of HER2-amplified cases in each manual category were 4.0% (0), 13.7% (1+), 71.4% (2+), and 75.0% (3+), and in each AQUA category were 9.5% (normal), 13.7% (intermediate), and 77.8% (high).

HER2 Expression on Normal Epithelium. We then assessed the level of HER2 expression on normal breast epithelium with use of automated analysis on a microarray. This epithelium was derived from normal ducts and/or lobules isolated from uninvolved breast tissue taken from 84 breast cancer patients. Consistent with previous studies using biochemical assays, our results demonstrated a low but detectable level of HER2 in normal epithelium, which was tightly grouped into a single peak with a mean of 5 and a SD of 1.5 (AQUA score; Fig. 1*A*; Ref. 6).

Automated Analysis of HER2 Expression in Breast Cancer. In contrast to the tightly grouped peak in normal epithelium, HER2 expression in breast tumors was broadly distributed (Fig. 1*C*). Expression levels of HER2 in tumors exhibited a mode similar to that of normal epithelium, but with significant skew toward higher-level expression. Examination of the histogram suggested that there were three naturally occurring populations based on HER2 expression: normal, intermediate, and high (Fig. 1*C*). A discernible break in the histogram at AQUA score 25 divided HER2-high from the remaining tumors. The remaining tumors could then be subdivided into HER2-low and HER2-intermediate groups depending on whether their expression levels were greater than the mean HER2 expression on normal epithelium + 1 SD (AQUA score <6.5; Fig. 1, *A* and *C*). On the basis of these divisions, 17.5% of the tumors were designated HER2 normal, 71.3% were HER2 intermediate, and 11.2% were HER2 high.

Comparison of Manual and Automated Techniques. We then compared HER2 expression as gauged by automated and manual techniques (Fig. 1, *panels C* and *B*, respectively). In contrast to AQUA scores, which were continuously scored on a scale of 0–255, manual scoring of HER2 expression was performed on a nominal four-point scale (0 to 3+). Despite this difference, regression analysis demonstrated good correlation between the two methods ($r = 0.704$). However, there was a significant degree of overlap in the automated scores of cases from adjacent manually determined groups (Fig. 1*D*). Whereas there was a clear division between the histograms of tumors scoring 0/1+ and 2+/3+, the distinction between tumors scoring 0 and 1+ was indistinct. This result shows the difficulty in manually translating a biological (continuous) marker into a nominal four-point scale. Even for the trained eye of a pathologist, accurate distinction between nominal categories (*e.g.*, 2+ *versus* 3+) is difficult and often arbitrary. Indeed, recent studies have demonstrated a significant lack of reproducibility in the clinical determination of HER2 levels attributable in part to this difficulty (7–9).

Examination of manual and automated techniques revealed that both were equally able to define a population of tumors expressing high levels of HER2 with poor outcome (relative risk, 2.25 and 2.18; $P = 0.0007$ and 0.0013, respectively; Table 1). However, unlike manual analysis, automated analysis revealed that tumors expressing normal levels of HER2 also showed a significantly worse outcome (relative risk, 1.71; $P = 0.0091$; Table 1). Given the amount of overlap in the 0 and 1+ categories from manual scoring (Fig. 1*D*), it is not surprising that manual assessment of stained slides has not previously identified the HER2-normal population.

Defining the Subpopulation of HER2-normal Tumors. To determine whether HER2 expression correlated with known prognostic markers in our cohort, we assessed possible associations between HER2 and hormone receptor status, tumor size, and nuclear grade. High-level HER2 expression was correlated with high nuclear grade and inversely correlated with estrogen receptor status (Table 2).

The HER2-normal population showed no significant correlation with nodal involvement, tumor size, or estrogen receptor, but did show an association with high nuclear grade ($P = 0.0494$; Table 2). Few of the HER2-normal tumors exhibited gene amplification (2 of 21 examined), ruling out the possibility that in tumors expressing

Table 1 *Univariate analysis of 30-year disease-related survival*

Marker	*n*	*P*	Relative risk	95% confidence interval
HER2 manual score		0.0071		
0	153		1.00	
1+	50	0.9383	1.02	0.68–1.52
2+	13	0.9763	1.01	0.49–2.08
3+	28	0.0007	2.25	1.41–3.58
HER2 AQUA score		0.0009		
Normal	46	0.0091	1.71	1.14–2.56
Intermediate	188		1.00	
High	30	0.0013	2.18	1.35–3.51
HER2 amplification (FISH)	22	0.8121	1.07	0.60–1.90
Nodal involvement		0.0279		
1–3	68		1.00	
4–9	54	0.6708	1.08	0.75–1.55
≥10	141	0.0086	1.62	1.13–2.33
Tumor size (cm)		0.0007		
<2	80		1.00	
2–5	53	0.1255	1.33	0.92–1.93
>5	102	0.0001	2.09	1.43–3.07
Nuclear grade				
High	95	0.0040	1.55	1.15–2.08
Estrogen receptor				
Negative	104	0.0262	1.41	1.041–1.906

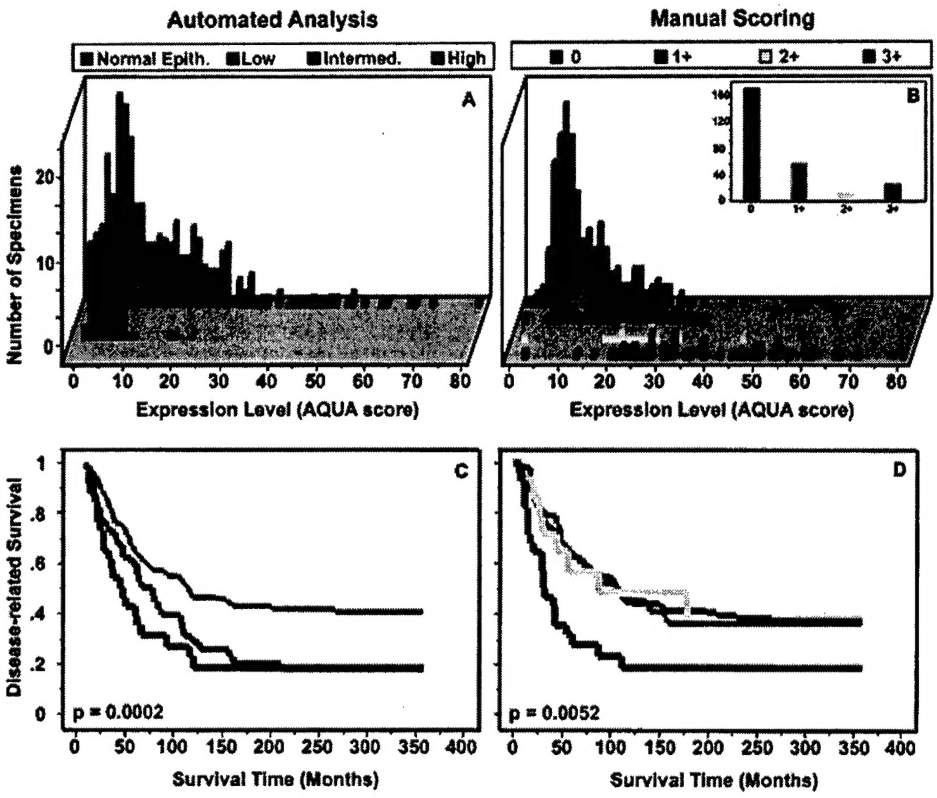

Fig. 1. Automated analysis of HER2 divides tumors into three categories based on their level of expression. *A*, analysis of 84 samples of normal epithelium demonstrates a low but detectable level of HER2 expression (*light blue*). Examination of a cohort of 300 node-positive carcinomas shows a right-skewed histogram (*dark blue*, *green*, and *red*). Cases were divided by expression level as follows: high (AQUA score >25; *red*), normal (AQUA score less than the mean expression of normal epithelium + 1 SD; *dark blue*), and intermediate (between normal and high; *green*). *B*, manual (visual) analysis of HER2 staining using a nominal four-point scale shows that 15% of the tumors over-express HER2 (2+/3+; *inset*). AQUA scores of tumors separated according to their manual score (0 to 3+) show significant overlap, particularly between 0 and 1+ tumors. *C*, Kaplan-Meier analysis of automated HER2 scores shows that both normal and high-level expressers do poorly relative to intermediate-level tumors. *D*, Kaplan-Meier analysis of manual HER2 scores distinguishes a survival difference only with the high (3+) expressers.

normal levels of HER2, the *HER2* gene is amplified but the HER2 protein is not detected.

Multivariate Analysis of HER2-normal and -high Populations. Finally, we determined whether normal or high expression of HER2 by tumors was an independent predictor of long-term disease-related survival. Combined multivariate analysis of HER2 with the traditional histopathological markers, nodal involvement, tumor size, nuclear grade, and estrogen receptor, demonstrated that both normal- and high-level HER2 expression were independently predictive of patient outcome (Table 3).

Our data suggest that HER2 divides cases of node-positive breast carcinoma into three categories: normal, intermediate, and high expressers. Tumors expressing either normal or high HER2 levels do poorly in long-term follow-up. Of particular note are three previous studies that have looked at HER2 expression levels using "gold standard" biochemical techniques (Western blots and ELISAs; Refs. 6, 10–13). Two of these studies suggested a bimodal distribution for HER2, with both low and high levels correlating with known markers of tumor aggression (10–12), but a third found no such distribution (13). Because such techniques require fresh tissue for analysis, they were unable to assess long-term follow-up on a large cohort of patients. The AQUA-based analysis provides quantitative information from tissue microarrays constructed from archival tissues; we thus were able to examine a large cohort of patients with known long-term disease-related survival. Our data show that normal HER2 expression is an independent prognostic indicator of poor outcome and demonstrate that, unlike manual immunohistochemical analysis, automated analysis can identify a patient population that is otherwise detectable only by established biochemical assays.

HER2 overexpression can induce an aggressive phenotype via the activation of downstream regulators (*e.g.*, phosphoinositol 3-kinase, *Erk*/MAP kinase, and *Ras*; Refs. 14–16). How normal levels of HER2 could be associated with a similar aggressive phenotype is unknown at present. We speculate that these tumors might overexpress another growth factor receptor that promotes tumor aggression via a ligand-dependent or -independent mechanism. It is possible that expression

Table 2 *Distribution of prognostic markers by HER2 level based on χ^2 analysis*

	All cases					$P(\chi^2)$	
Marker	*n*	%	Normal (%)	Intermediate (%)	High (%)	Normal *vs.* intermediate	High *vs.* intermediate
Nodes positive	268					0.8171	0.1891
1–3	145	54	60	54	43		
4–9	70	26	23	27	33		
≥10	53	20	17	19	23		
Tumor size (cm)	238					0.3033	0.8911
<2	102	43	35	44	48		
2–5	81	34	44	32	32		
>5	55	23	21	24	20		
Nuclear grade	269					0.0494	0.0011
High	97	36	45	30	60		
Estrogen receptor	263					0.5325	<0.0001
Negative	105	40	39	34	77		

Table 3 *Multivariate analysis of 30-year disease-related survival*

Marker	*n*	*P*	Relative risk	95% confidence interval
HER2		0.0097		
Normal	42	0.0191	1.68	1.09–2.59
Intermediate	162		1.00	
High	25	0.0136	1.96	1.15–3.36
Nodal involvement		0.1058		
1–3	60		1.00	
4–9	48	0.5915	1.12	0.73–1.72
≥10	121	0.0353	1.61	1.03–2.53
Tumor size (cm)		<0.0001		
<2	78		1.00	
2–5	52	0.2220	1.31	0.85–2.01
>5	99	<0.0001	2.59	1.67–4.02
Nuclear grade				
High	87	0.2158	1.26	0.87–1.82
Estrogen receptor				
Negative	89	0.0032	1.75	1.21–2.54

of such alternate growth factor receptors in some tumors results in the down-regulation of HER2 expression via a feedback mechanism, producing aggressive tumors bearing a HER2-normal phenotype. Another possible explanation for the poor prognosis of HER2-normal tumors is that high levels of coreceptor ligand-independent activation of HER2 might result in the internalization and degradation of the receptor, producing apparent low-level HER2 expression. Finally, HER2-normal breast cancers may represent a population of aggressive poorly differentiated neoplasms that have developed HER2- and growth factor-independent mechanisms for their growth. The association between normal HER2 expression levels and high nuclear grade supports this idea. Recent data from the Brown and Botstein group also support this finding. They showed five unique breast cancer classes by cDNA array clustering experiments, two of which had very poor outcomes. One of these groups was HER2 positive, but the other showed no evidence of HER2 overexpression (17).

From a clinical perspective, response to Herceptin has largely been seen in HER2 high expressers or HER2-amplified cases. This may be attributable to the fact that 2+ or 3+ levels of expression were required for entry into most clinical trials (18–20). The response of 0 or 1+ tumors to paclitaxel with and without Herceptin is being studied in a large randomized trial (CALGB 9840; Ref. 21). Although patients with HER2-normal tumors are unlikely to respond to Herceptin, they may benefit from more aggressive traditional chemotherapy. The ability to accurately distinguish between HER2-normal and HER2-intermediate tumors by automated analysis not only has prognostic value but may also help in the development and evaluation of new therapeutics targeted to treat this subpopulation.

Acknowledgments

We thank Michael DiGiovanna and D. Craig Allred for critical review of this manuscript. We also thank Nicole Parisot, Thomas D'Aquila, Mary Helie, Lori Charette, and Diana Fischer for assistance in this effort.

References

1. Camp, R. L., Chung, G. G., and Rimm, D. L. Automated subcellular localization and quantification of protein expression in tissue microarrays. Nat. Med., *8:* 1323–1328, 2002.
2. Rimm, D. L., Camp, R. L., Charette, L. A., Olsen, D. A., and Provost, E. Amplification of tissue by construction of tissue microarrays. Exp. Mol. Pathol., *70:* 255–264, 2001.
3. Kononen, J., Bubendorf, L., Kallioniemi, A., Barlund, M., Schraml, P., Leighton, S., Torhorst, J., Mihatsch, M. J., Sauter, G., and Kallioniemi, O. P. Tissue microarrays for high-throughput molecular profiling of tumor specimens. Nat. Med., *4:* 844–847, 1998.
4. Camp, R. L., Charette, L. A., and Rimm, D. L. Validation of tissue microarray technology in breast carcinoma. Lab. Investig., *80:* 1943–1949, 2000.
5. Torhorst, J., Bucher, C., Kononen, J., Haas, P., Zuber, M., Kochli, O. R., Mross, F., Dieterich, H., Moch, H., Mihatsch, M., Kallioniemi, O. P., and Sauter, G. Tissue microarrays for rapid linking of molecular changes to clinical endpoints. Am. J. Pathol., *159:* 2249–2256, 2001.
6. Dittadi, R., Donisi, P. M., Brazzale, A., Marconato, R., Spina, M., and Gion, M. Immunoenzymatic assay of erbB2 protein in cancer and non-malignant breast tissue. Relationships with clinical and biochemical parameters. Anticancer Res., *12:* 2005–2010, 1992.
7. Paik, S., Bryant, J., Tan-Chiu, E., Romond, E., Hiller, W., Park, K., Brown, A., Yothers, G., Anderson, S., Smith, R., Wickerham, D. L., and Wolmark, N. Real-world performance of HER2 testing—National Surgical Adjuvant Breast and Bowel Project experience. J. Natl. Cancer Inst. (Bethesda), *94:* 852–854, 2002.
8. Roche, P. C., Suman, V. J., Jenkins, R. B., Davidson, N. E., Martino, S., Kaufman, P. A., Addo, F. K., Murphy, B., Ingle, J. N., and Perez, E. A. Concordance between local and central laboratory HER2 testing in the breast intergroup trial N9831. J. Natl. Cancer Inst. (Bethesda), *94:* 855–857, 2002.
9. Zujewski, J. A. "Build quality in"—HER2 testing in the real world. J. Natl. Cancer Inst. (Bethesda), *94:* 788–789, 2002.
10. Koscielny, S., Terrier, P., Spielmann, M., and Delarue, J. C. Prognostic importance of low c-erbB2 expression in breast tumors. J. Natl. Cancer Inst. (Bethesda), *90:* 712, 1998.
11. Koscielny, S., Terrier, P., Daver, A., Wafflart, J., Goussard, J., Ricolleau, G., Delvincourt, C., and Delarue, J. C. Quantitative determination of c-erbB-2 in human breast tumours: potential prognostic significance of low values. Eur. J. Cancer, *34:* 476–481, 1998.
12. Dittadi, R., Brazzale, A., Pappagallo, G., Salbe, C., Nascimben, O., Rosabian, A., and Gion, M. ErbB2 assay in breast cancer: possibly improved clinical information using a quantitative method. Anticancer Res., *17:* 1245–1247, 1997.
13. Ferrero-Pous, M., Hacene, K., Tubiana-Hulin, M., and Spyratos, F. Re: Prognostic importance of low c-erbB2 expression in breast tumors. J. Natl. Cancer Inst. (Bethesda), *91:* 1584–1585, 1999.
14. Ben-Levy, R., Paterson, H. F., Marshall, C. J., and Yarden, Y. A single autophosphorylation site confers oncogenicity to the Neu/ErbB-2 receptor and enables coupling to the MAP kinase pathway. EMBO J., *13:* 3302–3311, 1994.
15. Amundadottir, L. T., and Leder, P. Signal transduction pathways activated and required for mammary carcinogenesis in response to specific oncogenes. Oncogene, *16:* 737–746, 1998.
16. Janes, P. W., Daly, R. J., deFazio, A., and Sutherland, R. L. Activation of the Ras signalling pathway in human breast cancer cells overexpressing erbB-2. Oncogene, *9:* 3601–3608, 1994.
17. Sorlie, T., Perou, C. M., Tibshirani, R., Aas, T., Geisler, S., Johnsen, H., Hastie, T., Eisen, M. B., van de Rijn, M., Jeffrey, S. S., Thorsen, T., Quist, H., Matese, J. C., Brown, P. O., Botstein, D., Eystein Lonning, P., and Borresen-Dale, A. L. Gene expression patterns of breast carcinomas distinguish tumor subclasses with clinical implications. Proc. Natl. Acad. Sci. USA, *98:* 10869–10874, 2001.
18. Vogel, C. L., Cobleigh, M. A., Tripathy, D., Gutheil, J. C., Harris, L. N., Fehrenbacher, L., Slamon, D. J., Murphy, M., Novotny, W. F., Burchmore, M., Shak, S., Stewart, S. J., and Press, M. Efficacy and safety of trastuzumab as a single agent in first-line treatment of HER2-overexpressing metastatic breast cancer. J. Clin. Oncol., *20:* 719–726, 2002.
19. Cobleigh, M. A., Vogel, C. L., Tripathy, D., Robert, N. J., Scholl, S., Fehrenbacher, L., Wolter, J. M., Paton, V., Shak, S., Lieberman, G., and Slamon, D. J. Multinational study of the efficacy and safety of humanized anti-HER2 monoclonal antibody in women who have HER2-overexpressing metastatic breast cancer that has progressed after chemotherapy for metastatic disease. J. Clin. Oncol., *17:* 2639–2648, 1999.
20. Slamon, D. J., Leyland-Jones, B., Shak, S., Fuchs, H., Paton, V., Bajamonde, A., Fleming, T., Eiermann, W., Wolter, J., Pegram, M., Baselga, J., and Norton, L. Use of chemotherapy plus a monoclonal antibody against HER2 for metastatic breast cancer that overexpresses HER2. N. Engl. J. Med., *344:* 783–792, 2001.
21. Seidman, A. D., Fornier, M. N., Esteva, F. J., Tan, L., Kaptain, S., Bach, A., Panageas, K. S., Arroyo, C., Valero, V., Currie, V., Gilewski, T., Theodoulou, M., Moynahan, M. E., Moasser, M., Sklarin, N., Dickler, M., D'Andrea, G., Cristofanilli, M., Rivera, E., Hortobagyi, G. N., Norton, L., and Hudis, C. A. Weekly trastuzumab and paclitaxel therapy for metastatic breast cancer with analysis of efficacy by HER2 immunophenotype and gene amplification. J. Clin. Oncol., *19:* 2587–2595, 2001.